Measurement 186 (2021) 110155

Contents lists available at ScienceDirect

Measurement

journal homepage: www.elsevier.com/locate/measurement

Nonlinear ultrasonic testing and data analytics for damage characterization: A review☆

Hongguang Yun [a], Rakiba Rayhana [a], Shashank Pant [b], Marc Genest [b], Zheng Liu [a,*]

[a] University of British Columbia, Okanagan Campus, Kelowna, British Columbia, V1V 1V7, Canada
[b] Aerospace Research Centre, National Research Council of Canada, Ottawa, Ontario, K1A 0R6, Canada

ARTICLE INFO

Keywords:
Nonlinear ultrasonic testing
NDT&E
Damage characterization
Machine learning
Neural network

ABSTRACT

Nondestructive testing and evaluation (NDT&E) are commonly used in the industry for their ability to identify damage and assess material conditions. Ultrasonic testing (UT) is one of the most popular NDT&E techniques. A variant of ultrasonic testing known as nonlinear ultrasonic testing (NUT) has some advantages over conventional (linear) UT as it is more sensitive to damages in their early stages; even at the microscopic levels. Furthermore, the nonlinear characteristics of ultrasonic waves can be correlated to several material properties. In the last two decades, the NUT method has been investigated from two aspects, namely the direct (modeling) problem and the inverse (NUT testing) problem. The direct problem aims to establish the nonlinear mechanism and analyze the behavior of wave-damage interaction. The inverse problem is investigated under three headings: (1) data acquisition with NUT techniques, (2) signal pre-processing and feature extraction, and (3) parameter analysis for damage characterization. The conventional data analytical methods extract nonlinear features from noisy signals and build a damage index to characterize damages. However, damage index-based analyzing model can be challenging, as other factors affect the overall system nonlinearity such as complex specimen geometry, different damage characteristics, varying ambient conditions, and measurement uncertainties. To overcome these shortcomings, machine learning (ML) methods appear promising for the analysis of complex nonlinear ultrasonic signals by exploiting data mining and pattern recognition capabilities. Therefore, this paper aims to provide a comprehensive review of the state-of-the-art ML-enriched NUT for damage characterization. Other NUT-based technologies are also reviewed, including modeling of wave-damage interaction, different NUT techniques for data acquisition, signal pre-processing methods, and damage index-based parameter analysis strategies for damage characterization. Major emphasis is placed on the application of ML methods for NDT&E applications. Additionally, future research trends on data augmentation, complex damage characterization, and baseline-free methods using NUT are also discussed.

1. Introduction

In recent years, the demand for damage characterization in materials/structures has been growing to ensure a high level of performance and safety. In various industrial applications, such as aerospace, nuclear, defense, oil and gas, etc., knowing the condition of the materials is crucial for safe operations [1,2]. Early damage detection can improve efficiency and lower maintenance cost of the equipment [3]. The Non-Destructive Testing and Evaluation (NDT&E) are widely used for damage characterization without altering the performance of the materials under investigation.

There are several NDT&E techniques such as: visual inspection, ultrasonic testing (UT), infrared thermography, laser shearography, etc. UT is one of the most commonly used techniques for material characterization [4] and has been divided into conventional (linear) and nonlinear UT (NUT) in this paper. The conventional UT is established based on linear theory using the changes in amplitude, velocity, and phase of the ultrasound to assess material conditions [5]. However, several studies have revealed that early degradation and damage in materials (such as micro-cracks and delaminations) are sources of nonlinearity and can be detected using NUT techniques [6–8].

The study of NUT over the past two decades falls under two aspects, namely the direct (modeling) problem and the inverse (NUT testing) problem. The direct problem focuses on establishing nonlinear mechanism of wave-damage interaction. The inverse problem is implemented under three themes: (1) data acquisition with NUT techniques,

☆ This document is the results of the research project funded by the National Research Council of Canada (Grant No. 943411).
* Corresponding author.
E-mail addresses: hongguang.yun@ubc.ca (H. Yun), zheng.liu@ubc.ca (Z. Liu).

https://doi.org/10.1016/j.measurement.2021.110155
Received 1 May 2021; Received in revised form 2 September 2021; Accepted 5 September 2021
Available online 20 September 2021

(2) signal pre-processing and feature extraction methods, and (3) parameter analysis for damage characterization. Research on nonlinear ultrasonics can be traced back to the 1960s' [9] when the theoretical foundation of ultrasound propagating in fluids was established. Frouin et al. [5] were one of the first to examine the advantages of NUT for fatigue damage characterization. Experiments on metallic coupons showed that the second harmonic induced by material nonlinearity tends to increase by 180% as the fatigue damage develops. Research conducted by Bermes [10] showed the potential of using nonlinear Lamb waves to evaluate inherent material nonlinearity. A large and growing body of literature has investigated the effectiveness of using NUT for damage characterization. Specifically, different types of damages that can be detected using NUT, which include: fatigue crack [11] and corrosion [12] in metals, as well as, delamination [13], impact damage, and crack in composites [14]. A number of researchers have also evaluated the performance of NUT to detect damage in specimens with different geometries, such as: plates [15–17], pipes [18–20], and irregular shaped structures [21–23].

NUT has made a great stride in the NDT&E field, but there are still several shortcomings that impede the deployment of NUT in real industrial applications. First, current theoretical studies on the nonlinear mechanism are unable to encompass the entire materials nonlinearity phenomenon. Assumptions and simplifications are unavoidable in establishing a theoretical or numerical model of wave-damage interaction, which limits the theoretical analysis to model all nonlinear phenomena in the acquired wave signals. Second, many NUT methods fail to consider the influence of measurement and time-varying ambient conditions, which would further lower the confidence of signal analysis in a real industrial application. Third, existing NUT methods are not suited for real-time monitoring, due to the fact that (1) real-time monitoring requires robust methods which can adapt to the little difference between specimens and deterioration of machines; and (2) expertise for data analysis and post-processing are required for damage characterization.

To overcome the aforementioned shortcomings, a promising way is to apply machine learning (ML) methods to analyze NUT data. ML methods have demonstrated great advantages in extracting relevant and useful information from high-dimensional feature space. In the context of NUT for damage characterization, the use of ML methods can recognize complex and various nonlinear patterns and can reduce the uncertainties introduced by time-varying ambient conditions. For example, Ren et al. [24] considered the effects of temperature on the damage characterization of composites by updating the model to fit the time-varying conditions using Bayesian inference. ML methods have been validated with automated pattern recognition and decision-making abilities for real-time monitoring applications [25,26].

Damage characterization tasks can be classified into damage detection, damage localization, and damage quantification. Several attempts have been made to address these damage characterization tasks using ML-enriched NUT techniques. For the most basic damage detection task, a support vector machine (SVM) could identify damage with 95% accuracy as shown by [27], where a two stage automatic detector was proposed to identify the notch damage in an aluminum plate specimen. Probabilistic technique based on the Bayesian theorem [28,29] has been deployed for damage localization and quantification, a precise prediction can be obtained by reducing uncertainties during the measurement and data analysis process. Lim et al. [17] proposed to build an artificial neural network (ANN) model to predict the crack length, where the error of the estimated crack length was within 2 mm. In the last few years, the use of the convolutional neural network (CNN) has shown a promising way to characterize damage without requiring handcrafted nonlinear features [30,31].

To date, several reviews have been published in the context of NUT for damage characterization. Jhang [4] reviewed the most commonly used NUT techniques for micro-crack characterization. Broda et al. [32] summarized the physical mechanism of wave-crack interaction in solids. Marcantonio et al. [33] compared and summarized different testing and analyzing strategies concerning various types of damages including corrosion, fatigue, and thermal damage. Although existing reviews provide massive information and useful insights, most published investigations are limited to local surveys and no previous study has investigated the application of ML methods in the context of NUT. For example, Matlack et al. [34] did a comprehensive review mainly on the topic of second harmonic generation and corresponding applications. Guan et al. [35] and Ghavamian et al. [36] separately investigated the application of using guided waves in the pipeline for damage characterization. Most ML-enriched NUT studies were published in the last five years, but an in-depth review for implementing ML methods to NUT data for damage characterization is missing in the available literature.

To address the aforementioned gaps, this paper is set out to review the NUT technology and state-of-the-art data analytics methods, where the focus is placed on the ML-enriched damage characterization methods. The contributions of this review paper can be summarized as follows:

1. **NUT framework for NDT&E:** A framework using NUT techniques for damage characterization is proposed. The theoretical studies of nonlinear mechanisms are used to provide knowledge on building an ML model for damage characterization. And the NUT and ML methods are bridged at the signal pre-processing and feature extraction steps.
2. **Comprehensive review:** A comprehensive investigation of ML methods and applications for damage characterization using NUT is conducted.
3. **Future directions:** Current challenges faced by the NUT techniques and corresponding future research directions are discussed.

This paper is structured as follows: Section 2 outlines the NUT technologies for damage characterization, including the modeling of nonlinear wave-damage interaction, NUT techniques, and applications into damage characterization. Next, the NUT signal pre-processing and parameter analysis methods are reviewed in Section 3. Emphasis is placed on the introduction and application of ML methods for analyzing NUT data. Section 4 discusses the future research directions using ML methods for NUT. Finally, the conclusions of this paper are provided in Section 5.

2. Nonlinear ultrasonic testing technology

2.1. Overview of research on NUT technology

Research on NUT technology for damage characterization in solid materials can be divided into the direct problem and the inverse problem. The direct problem is defined as the mathematical modeling of wave-damage interaction in the specimen. Based on the findings from the direct problem studies, the research of inverse problem aims to inspect the specimen using NUT techniques for damage characterization. As listed in Table 1, in the direct problem setting, the input of the model includes the specimen and damage properties, ultrasonic wave properties, and optional artificial noise. The output is the expression of propagating ultrasonic waves and nonlinear phenomena induced by damages and boundaries in the specimen. In the inverse problem setting, the input is the specimen properties and sensory signals; whereas, the output could be the indication of damage, damage properties, and remaining useful life prediction.

Given the inputs and expected outputs of two types of problems, Fig. 1 illustrates the research contents and procedures of using NUT technology for damage characterization. The direct problem is concerned with the ultrasonic wave propagation behaviors, wave-damage interaction mechanism, and corresponding nonlinear phenomena. For

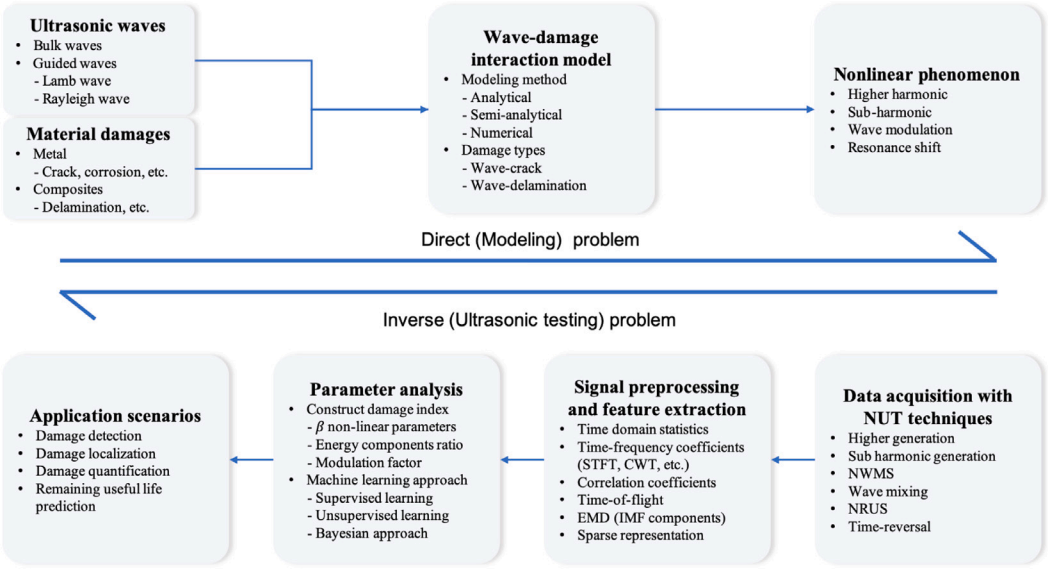

Fig. 1. Flowchart of the direct and inverse problem for damage characterization using NUT.

Table 1
Direct and inverse NUT problems.

Direct problems	Inverse problems
Theoretical input data:	**Experimental input data:**
• Specimen properties	• Specimen properties
• Damage properties	• Sensory ultrasonic wave signals
• Ultrasonic wave properties	
• Noise (optional)	
Outputs:	Outputs:
• Wave propagation	• Specimen properties
• Wave-damage interaction mechanism	• Damage exists or not
• Nonlinear phenomena	• Damage location
	• Damage size/shape
	• Remaining useful life prediction

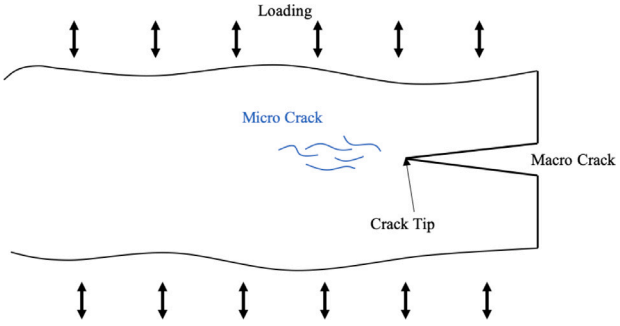

Fig. 2. Formation process of micro-crack in metallic materials.

example, assuming that ultrasonic waves with fundamental frequency propagate in the specimen with micro-crack damage, the micro-crack will induce higher harmonics as ultrasonic waves propagate through the crack. The well-known nonlinearity parameter β, which is defined based on the ratio of the amplitude of higher harmonics to that of fundamental harmonic as an indicator of damage presence [5]. The existing literature has shown that the β parameter only increases monotonically when the crack is small [37,38]. Generally, the β parameter tends to increase when the damage is at its early stage and then decreases as the damage grows. Section 2.2 provides the reviews of modeling of wave-damage interaction and summaries the resulting nonlinear phenomena.

Following the direct problem research, a large volume of published methods are developed to solve the inverse problem. As shown in Fig. 1, the inverse problem is carried out in the following sequence, namely (1) data acquisition with NUT techniques, (2) signal pre-processing and feature extraction, and (3) parameter analysis for damage characterization. First, the NUT is performed to inspect the specimen and collect the wave signals. The sensory ultrasonic waves require signal pre-processing to extract nonlinear features. A variety of signal pre-processing techniques are described in Section 3.1. The parameter analysis is then carried out to interpret the extracted nonlinear features and evaluate the damage conditions. The conventional parameter analysis method characterize damages by building a damage index (DI) such as the nonlinearity parameter β. However, DI-based methods are vulnerable to complex inspection scenarios and time-varying ambient conditions. Instead, with the powerful data mining and pattern recognizing abilities, ML-based parameter analysis methods can capture complicated nonlinear features and map them to the damage conditions. Many recent studies have shown the effectiveness of using ML methods for damage detection [27], localization [39], and quantification [40]. Section 3 presents the state-of-the-art parameter analysis methods.

2.2. Nonlinear mechanism of wave-damage interaction

The linear UT techniques utilize dissipation of wave energy due to attenuation, reflection, and change of phase to characterize damages [41]. However, these linear features are insensitive to microscopic damages such as micro-cracks and delamination [5]. This is because the physical mechanism of micro damage wave interaction is full of nonlinearity [42]. A major difference between linear UT and NUT is that in the latter the presence of damages would generate new frequency harmonics [4].

Ultrasonic waves can be divided into bulk waves and guided waves. Longitudinal and shear waves are the two modes of bulk waves that are widely used in UT. The particle oscillation direction of the longitudinal and shear wave is parallel and transverse to the wave propagation direction, respectively. Guided wave on the other hand consists of three modes — Rayleigh, shear-horizontal, and Lamb waves. Rayleigh wave is also known as a surface wave for propagating near the free surface and has been used for surface damage detection. Shear-horizontal wave is particularly used in damage characterization in adhesive bonds and laminated composite plates [43–45]. Lamb wave, which is made up of a superposition of longitudinal and shear modes is the most widely used

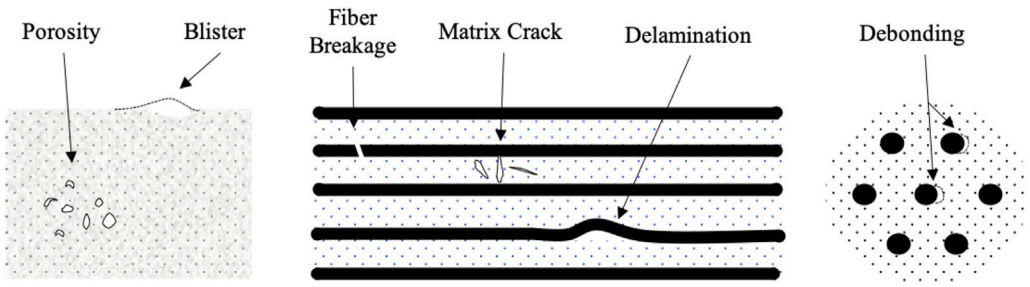

Fig. 3. Various types of damages in multi-layer composite materials.

guided wave. Although Lamb wave is multi-modal and dispersive, it provides an attractive solution for detecting damage in thin plates and shell-like structures, as well as, for its ability to propagate over long distances covering a larger inspection area.

Without loss of generality, two representative direct problem schemes as shown in Table 2 are selected to demonstrate the modeling of wave-damage interaction in metallic and composites materials, respectively. It has been reported that cracks account for most of the failures in metallic materials [46]. As shown in Fig. 2, the crack growth process is stochastic and difficult to predict. Therefore, it is important to detect a crack in its early stage. Most metallic structures can be treated as isotropic with regard to wave propagation. In which case, the result of wave-damage interaction can be obtained by solving the analytical wave equation. Compared with metallic structures, composite structures have very complex wave propagation characteristics due to their anisotropic nature. And thus the numerical modeling method is preferred instead of solving the analytical wave equation. Fig. 3 shows typical damages found in multi-layer laminate composite. Since delamination is one of the most common damage types in a composite structure, it has been selected to illustrate the wave-damage interaction in a composite material.

2.2.1. Wave-crack interaction

Elastic nonlinearity. The presence of elastic nonlinearity can be explained by introducing high-order terms in the Hooke's Law. For the free energy in the power series [47],

$$F = F_0 + \frac{1}{2}\lambda u_{ii}^2 + \mu u_{ik}^2, \tag{1}$$

where F is the force, F_0 is the initial force, λ and μ are Lame constants and u_{ik}^2 is the deformation tensor that can be described as [32]:

$$u_{ik} = \frac{1}{2}\left(\frac{\partial u_i}{\partial x_k} + \frac{\partial u_k}{\partial x_i}\right) \tag{2}$$

To consider the nonlinear behavior, a higher order is included in the displacement tensor u_{ik}, which becomes:

$$u_{ik} = \frac{1}{2}\left(\frac{\partial u_i}{\partial x_k} + \frac{\partial u_k}{\partial x_i} + \frac{\partial u_l}{\partial x_i}\frac{\partial u_l}{\partial x_k}\right) \tag{3}$$

leading to the quadratic terms, which produce higher harmonic frequency in the spectrum [48].

This quadratic stress–strain relation is a simplified model and cannot provide an explanation for some phenomena, such as sub-harmonic. It was reported that under a rapidly changing loading, the stress–strain in rock follows the elastic hysteresis, where the relation is different in the loading as compared to the unloading stage, as shown in Fig. 4. The nonlinearity derived from hysteresis is similar to the cubic elastic nonlinearity, with the result of odd higher harmonic generation in the spectrum [49]. More studies about elastic hysteresis can be found in the review paper by Broda et al. [32].

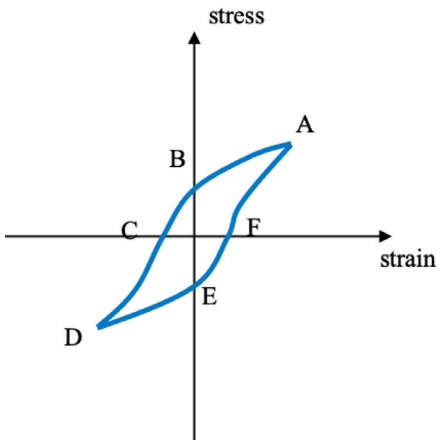

Fig. 4. The stress–strain relation of materials with an elastic hysteresis mechanism.

Contact nonlinearity. The stress–strain relation model only reveals the nonlinearity of the materials but does not consider the local interaction of ultrasonic waves and damages. Bi-linear stiffness is a simplified theory that describes the behavior of wave-crack interaction. As shown in Fig. 5, with an alternating external loading applied to the specimen, the crack would keep switching between opening and closing, causing the global stiffness change. The most popular model based on the bi-linear stiffness describing the behavior of the crack is the so-called "breathing crack" [50]. When an ultrasonic wave propagates through the crack, it acts as alternating loading, making the crack in a state of alternating tension and compression. In a compression state, the crack is closed and the stiffness does not change; whereas, in a tension state, the crack is open reducing the local stiffness [51,52]. This phenomenon is termed contact acoustic nonlinearity (CAN). Fig. 6 illustrates the mechanism of the breathing crack due to propagating ultrasonic waves. As the consequence of ultrasonic waves propagating through a breathing crack, sub and higher harmonics will appear in the frequency spectrum [53,54] and the fundamental wave signal will be altered by the presence of crack [55–57].

The bi-linear model provides a simplified description of the crack contact. However, the crack surfaces are usually rough, and thus only parts of crack surfaces are in contact with each other or in contact with the propagating ultrasonic waves. To make the model closer to reality, researchers have built more complex models. For example, Hertz's theory was introduced to establish a crack model, where a crack is considered as two elastic frictionless half spaces [6,58]. Johnson and Johnson [59] used the sinusoids to describe the shape of the rough surfaces based on the statistics. Greenwood and Williamson [60] divided the general contact surface into multiple small single contacts with the same radius of curvature, which were randomly distributed along the surface. Although there are no new signal components found by establishing these complex models, they can give a better explanation of the nonlinear phenomena mentioned in the bi-linear model.

Table 2
Two representative schemes of nonlinear ultrasonic wave-damage interaction model.

Scheme	Wave-crack interaction	Wave-delamination interaction
Ultrasonic wave type	Bulk wave	Lamb wave
Modeling method	Analytical modeling	Numerical modeling
Medium property	Isotropic	Anisotropic

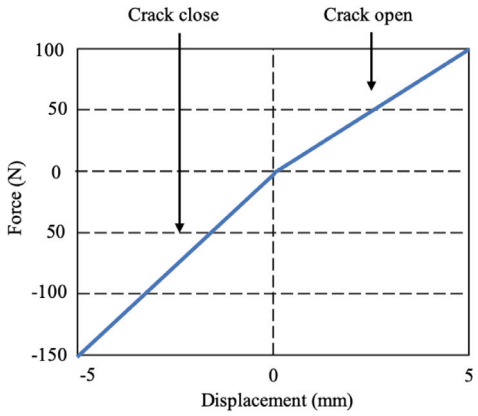

Fig. 5. The force–displacement relation of crack under Bi-linear model.

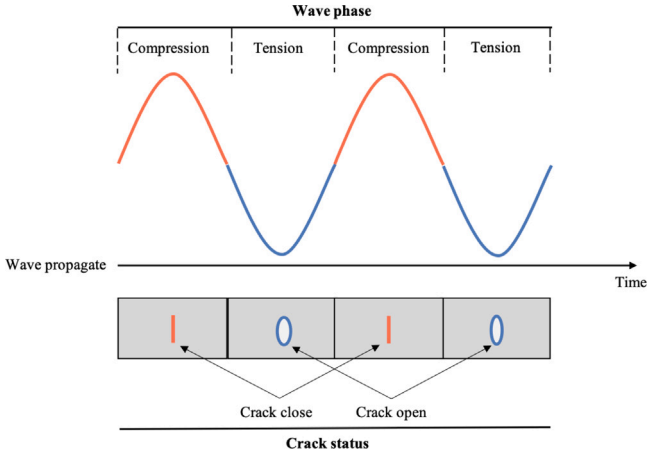

Fig. 6. Schematic illustration of breathing crack behavior due to propagating ultrasonic wave.

2.2.2. Wave-delamination interaction

The exact analytical solution of Lamb wave propagation in materials can be generated by using 3-D elasticity or can be approximated by laminated plate theory. Considering the interaction of wave damage in multi-layer composite laminates, it is difficult to obtain an analytical solution of wave-damage interaction due to anisotropic nature [61,62]. Thus, most researchers studied the interaction of wave-delamination using semi-analytical or numerical modeling methods. These techniques involve three fundamental processes, namely transducer modeling, wave propagation modeling, and damage modeling [63]. The most representative numerical model is based on the finite element method (FEM) for its ability to model complex structures and adaptability for industrial application [64]. Many other methods have been proposed to simulate the wave propagation process, such as the local interaction simulation approach (LISA) [65]. LISA requires a fine mesh of elements with small-time increments making it computationally intensive. Spectral methods, including frequency-domain spectral finite method (FSFE) [66] and time-domain finite spectral method (TSFE) [67], are proposed to overcome this limitation by using higher order interpolation of wavefield [68]. The use of Lamb waves introduce many other nonlinear phenomena including scattering and mode conversion:

1. Scattering. Murat et al. [69] built a 3-D FEM model to investigate the scattering phenomena of A_0 Lamb wave mode due to the presence of delamination with different geometries. Both simulation and experimental results showed that the scattering pattern was not affected by the shape of the delamination. However, the propagation direction and magnitude were altered by the width and depth of the delamination. Munian et al. [68] studied the effects of different depth, size, and position of the delamination on the near field and wave traveling off-axis. It was found the wave frequency close to the inherent resonance frequencies of laminates can be used to estimate the characteristics of the delamination. They also [70] studied guided wave propagation characteristics in multi-layer curved composite structures and found that the attenuation of reflected waves depends on the ratio of wavelength to the radius of curvature.
2. Mode conversion. Ramadas et al. [71,72] studied the interaction of Lamb waves with different delamination types in a plate using a FEM model. It was found that when the A_0 model is introduced at the entrance of the delamination, a new S_0 mode would be induced. In the presence of asymmetrical delamination, the newly generated model can propagate in both main and sub-laminates, whereas in the case of symmetrical delamination, it only propagates in sub-laminates.

2.3. NUT system

In the inverse problem, NUT is first performed to inspect specimens and collect wave signals containing the nonlinear features induced by damages. In this part, a general UT configuration is described and various NUT techniques are reviewed.

2.3.1. Basic UT configuration

A basic NUT setup can be characterized into three main configurations as shown in Fig. 7: (a) pulse-echo, (b) pitch–catch, and (c) through-transmission. The pulse-echo method uses one transducer, which acts as a transmitter to emit the waves and also as a receiver to capture echoes from the damage and specimen boundaries. Pitch–catch method uses two identical transducers — one to emit the ultrasonic waves and the other to receive the reflected pulses. The through-transmission method uses two transducers located on the opposite sides of the specimen.

A single-point measurement can only inspect the specimen along the wave propagation path. To cover all areas of the specimen, scan methods including A-Scan [73], B-Scan [74], and C-Scan [75] are developed. As shown in Fig. 8, the A-scan shows the relation of the signal strength and the time-of-flight (ToF) of the received ultrasonic waves. Compared to A-scan, B-scan adds the position information of the received waves and provides a profile view of the specimen. In the B-scan, the ToF of the waves and the position of the transducer are displayed along the vertical and horizontal axis, respectively. In the A-scan and B-scan modes, the movement of the transducer is one-dimensional; whereas, in C-scan mode, the transducer moves on a two-dimensional plane, which provides a plan view of the position and strength information of the received ultrasonic signal.

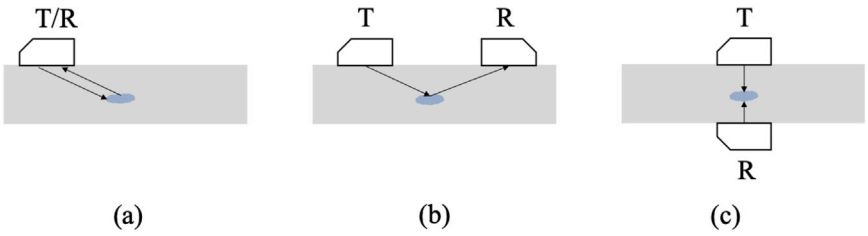

Fig. 7. Illustration of three types of transducer arrangement for UT: (a) Pulse-echo, (b) Pitch–catch, and (c) Through-transmission, T denotes transmitter and R denotes receiver.

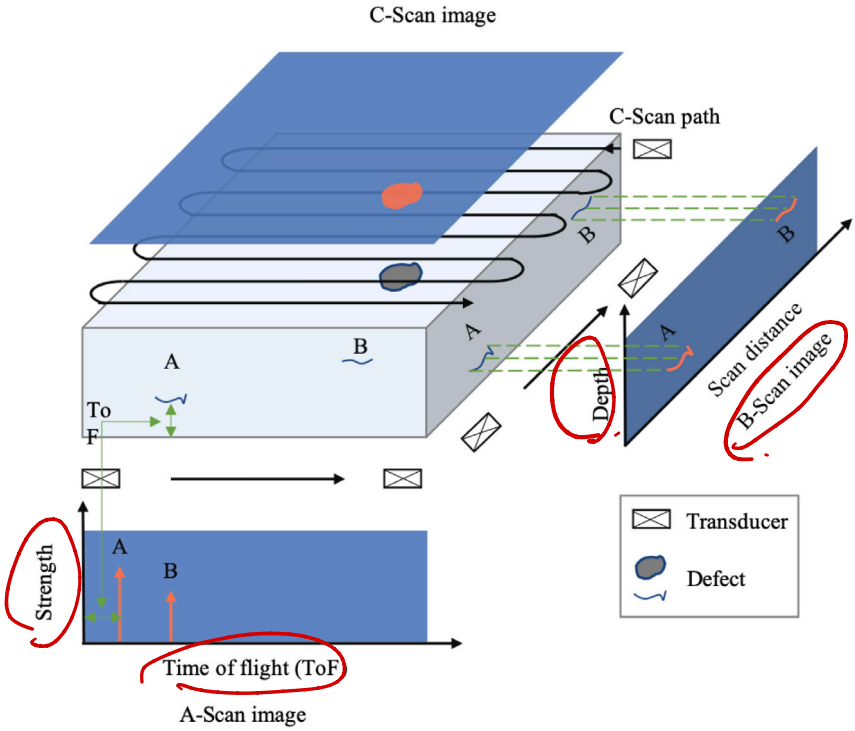

Fig. 8. A-scan, B-scan, and C-scan inspection using a pulse-echo UT configuration.

2.3.2. NUT techniques

Extra harmonics generation. The most commonly used NUT technique is the generation of higher harmonics (HH). As mentioned in Section 2.2, both material nonlinearity and contact nonlinearity can generate HH. The energy of HH waves originates from the fundamental wave component. As the order of the harmonics increases, the energy of the signal decreases significantly. And thus only the second-order harmonic is considered to evaluate nonlinearity in the real application. Naturally, sub-harmonic generation is also developed as a NUT technique according to the specimen's properties. The spectrum characteristics of HH and sub-harmonic generation methods are illustrated in Fig. 9. In addition to the original fundamental frequency, high-order frequency and sub-frequency harmonics will appear in the spectrum.

Nonlinear elastic wave spectroscopy. Inspired by the contact nonlinearity mechanism of the wave-damage interaction, damages can be regarded as the modulation source of the signal. Nonlinear elastic wave spectroscopy techniques were developed to characterize damages using the modulation characteristics. The most commonly used one is the nonlinear wave modulation spectroscopy (NWMS), which was designed according to the breathing crack model as mentioned in Section 2.2. During an NWMS inspection, two signals carrying different frequencies are introduced to the specimen, one is an ultrasonic wave with a high frequency denoted as f_h, the other is a vibration wave with a lower frequency denoted as f_l. The vibration signal is used to open the crack during tension and keep the crack closed during the compression phase. The amplitude of the ultrasonic signal will increase and decrease periodically as the crack shifts between the closed and open conditions, respectively. Thus, the ultrasonic signal is modulated by the vibration. As a result, a sideband will appear around the f_h with the frequency interval f_l in the spectrum.

Another wave modulation technique is called wave mixing, which uses two ultrasonic waves as the input signal instead of vibration signal in the NWMS technique. The nonlinear wave mixing technique exploits the interaction of the ultrasonic waves with each other when propagating in the medium because of the material nonlinearities [76]. A new wave will generate with the frequency equals to the sum or difference of the two incident waves. It has been reported that there are two major advantages of wave mixing over commonly used HH generation [77], which are: (1) it is much easier to extract the nonlinear mixing frequency as it is a different mode compared to the incident wave, and (2) wave mixing has the capability to measure the system nonlinearity by summing the response of the incident waves introduced separately without the presence of the interaction.

Considering the material hysteresis, the stress–strain relationship will change according to the amplitude of the excitation ultrasonic waves. If the wave amplitude increases, the modulus of the material decreases, causing an increase in the wave attenuation [8]. This phenomenon is also referred to as the shift of the resonance and the corresponding NUT technique is called the nonlinear resonant ultrasound spectroscopy (NRUS). Fig. 10 displays the spectrum characteristics of (a) NWMS, (b) wave mixing, and (c) NRUS.

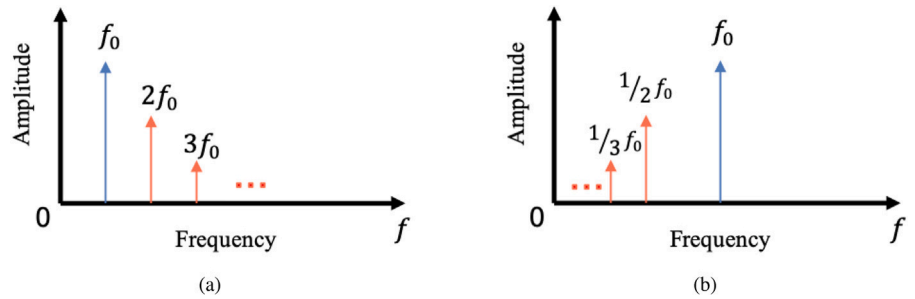

Fig. 9. Spectrum characteristics of extra harmonic generation methods: (a) Higher harmonic generation, (b) Sub-harmonic generation.

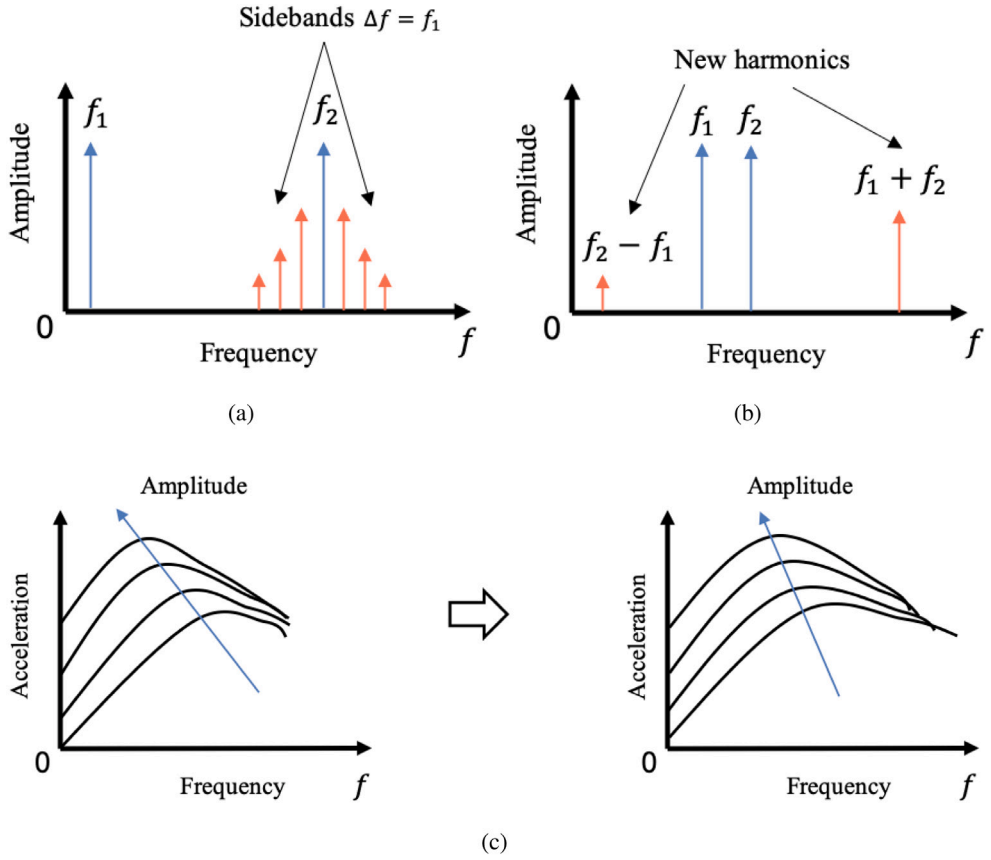

Fig. 10. Spectrum characteristics of nonlinear elastic wave modulation methods: (a) NWMS, (b) Wave mixing, (c) NRUS.

Time reversal. The last two decades have seen a growing trend towards utilizing the time reversibility of a Lamb wave to mitigate its need for baseline. Time reversal was developed to increase Lamb wave resolution at the beginning but was later applied for damage detection [78]. The procedure of time reversal is illustrated in Fig. 11. First, a tone burst Lamb wave is emitted from transducer A and the signal is recorded by transducer B after propagating through the medium. Then, the received signal is time-reversed in the time domain and emitted from transducer B to A along the same propagation path. At last, the received signal at transducer A is compared to the original signal. The linear reciprocity of a pristine structure will not be valid with the presence of damage making the received signal different from the original one.

Wang et al. [79] investigated the applicability of time reversal using guided waves in plates from the theoretical and experimental points of view. Their study showed that time reversal temporal and spatial focusing can be achieved with a distributed network of sensors and actuators. Since the work of Wang, the study of time reversal has gained momentum and was applied in various damage detection applications. Three avenues of time reversal are of particular interest, which are time reversibility investigation, testing technique improvement, and DI construction.

1. **Time reversibility investigation.** Park et al. [80] discussed the difficulty in reconstructing the time reversed signal because of the frequency-dependent property of the time reversal operator and proposed to use a narrowband excitation signal to alleviate this problem. Furthermore, they [81] examined the effect of various testing parameters including the dispersive and multi-modal nature of Lamb waves and medium boundaries on the time reversed reconstructed signal. Blanloeuil [82] validated the time reversal invariance when ultrasonic waves interact with a contact interface through a 2-D FEM model. Falcetelli et al. introduced a frequency compensation transfer function to better reconstruct the time reversed signal [83].
2. **Testing technique improvement.** Many researchers have sought to improve the time reversal process. Watkins and Jha

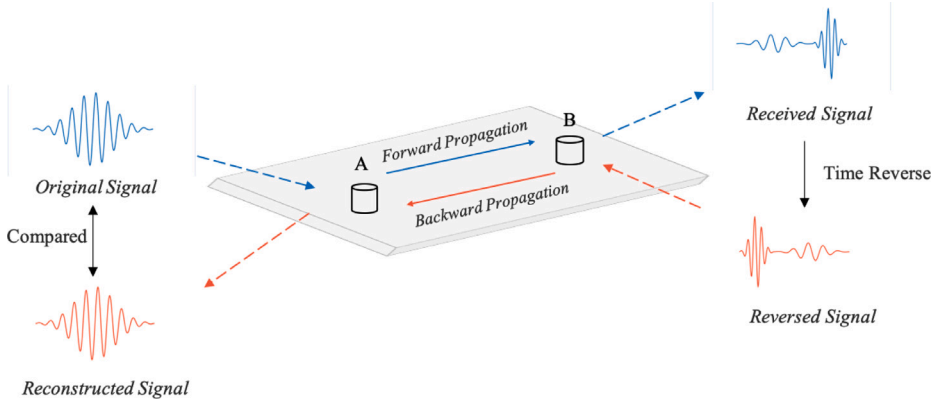

Fig. 11. Time reversal technique using a pitch–catch configuration.

[78] used only one transducer and can obtain an identical reconstructed signal compared to the traditional time reversal. Huang et al. [84] proposed to add an adaptive window function to the excitation signal and reconstructed signal to reduce the signal distortion. It was found that the time reversal process can be improved by processing the signal in frequency domain [85,86].

3. **DI construction.** Traditionally, the difference between the original excitation signal and the reconstructed signal is used to indicate damage presence. Commonly used DIs are based on correlation coefficients, change in amplitude or energy, and L_2 error norm [80,87]. However, it has been reported that some statistical-based DIs such as correlation coefficients does not provide reliable prediction regarding damage presence and growth [88,89].

2.4. Applications of NUT

The use of NUT techniques requires consideration of the material and damage properties according to their nonlinear characteristics. HH and sub-harmonics NUT techniques have similar implementation logic, in both cases extracting new harmonic components to indicate the presence of damages. Frouin et al. [5] conducted the HH technique to evaluate fatigue growth in titanium alloy with a through-transmission configuration using longitudinal waves. The experiment validated the generation and increase in the second harmonic as the damage grows. Walker et al. [90] used Rayleigh waves to characterize steel specimen using the HH method, which validated the relationship between material nonlinearity and the early stage of plastic deformation. The HH generation technique is also effective with Lamb waves. The second harmonic Lamb modes would increase cumulatively if the fundamental and second harmonic frequency propagate at an equal phase velocity [91]. This characteristic of Lamb waves is called the generation of cumulative second harmonics and it was experimentally validated by Bermes et al. [92]. Interested readers about second harmonic generation techniques are referred to Matlack et al. [34] for a comprehensive review.

To overcome the problem of low signal to noise ratio (SNR) of HH when the crack is partially closed, Yamanaka et al. [93] found that the physical properties and size of closed crack can be estimated by comparing the measured sub-harmonic waveforms with theoretical baseline. Ohara et al. [94,95] utilized the sub-harmonic techniques with a phased array configuration for closed crack evaluation. Their experimental results on aluminum alloy specimens demonstrated that the sub-harmonic technique outperformed the HH in locating and sizing the closed cracks. The measurement error of using sub-harmonic to quantify closed fatigue and corrosion cracks was around 1 mm. Subsequently, they [96] proposed an amplitude difference method to distinguish the sub-harmonics induced by closed crack and linear scatter when a short-burst wave is used. Likewise, Zhang et al. [97] studied the threshold of sub-harmonics induced by fatigue crack and boundaries. Experiments on an aluminum plate showed that fatigue crack would excite stronger nonlinear sub-harmonics compared to the boundaries. Ginzburg [98] applied the sub-harmonic technique to detect a 20 mm width disbonding in an adhesive joint.

The wave mixing technique can be classified into collinear wave mixing and non-collinear wave mixing according to the propagation directions of two incident ultrasonic waves [99]. Croxford et al. [77] applied the non-collinear wave mixing to assess plasticity and fatigue damage in aluminum alloy. A DI based on the normalized amplitude of the newly generated wave was constructed to quantify the damage severity. Jiao et al. [99,100] utilized the non-collinear wave mixing to quantify fatigue damage on different specimens. Various signal preprocessing methods including time domain, time–frequency domain, and bi-spectrum were used to characterize the fatigue cracks. Several studies have employed the collinear wave mixing technique to detect plastic deformation [101], crack in steel beam [102], crack in thin structures [103], and corrosion in stainless steel [104], etc.

Much of the current literature on wave mixing technique uses guided waves as the incident signal. Li et al. [105] simulated the mixing of a pair of A_0 and S_0 mode waves in thin plates, where the simulation result showed the nonlinear parameter increase monotonously along with the damage growth. Later, they [106] applied the guided wave mixing technique to characterize impact damage in composites, where they were able to detect circular impact damage with a diameter of 8 mm. Metya et al. [107] inspected the localized deformation due to creep in steel using the Lamb wave mixing technique, where they found that the amplitude of the frequency component would increase when the specimen was damaged by about 50%. There are also researchers who have implemented the wave mixing technique to locate microcracks in thin plates [108,109]. Simulation results showed that the length of damage location can be estimated with errors less than 2% when the crack length is about 60 mm.

Most of the applications of NRUS for damage characterization are used on granular materials such as rocks since the hysteresis effect is relatively strong. Van et al. [110] used NRUS to detect damage in slate tiles. The experiments showed that the NRUS outperforms the HH technique when hysteresis is the main driver of material nonlinearity. A number of studies have examined the effectiveness of using NRUS on identifying thermal damage [111,112], alkali–silica reaction damage [113,114] in concrete and damages in carbon fiber reinforced polymers (CFRP) [115]. In addition, Hogg et al. [116] applied the NRUS technique to the stress corrosion cracking characterization in stainless steel rods.

Gangadharan et al. [88] examined the time reversal behavior using fundamental symmetric and asymmetric Lamb waves for damage detection on an aluminum plate. The experiment showed using a broadband excitation signal provides a better resolution compared to a narrow band signal in detecting and locating damages. The time

reversal technique has been used in damage detection in composite structures [80,87,117], rod-like structure [118], corrosion monitoring in the pipeline [119], etc. Xu et al. [120] demonstrated the effectiveness of time reversal to detect damage in a pipeline, where a linear correlation was found between the peak values of the reconstructed signal and the degree of corrosion damage.

Table 3 summaries the experimental and industrial application of the aforementioned NUT techniques for damage characterization in various materials. In summary, HH is one of the most commonly used NUT techniques to identify damage in the specimen source of material nonlinearity. Sub-harmonic generation is suitable for closed crack detection and quantification. It is reported that collinear wave mixing is a promising method to assess the plastic deformation and fatigue damage in metallic materials [100]. It is worthy to note that the bispectrum shows great potential in extracting the nonlinearity-related harmonics. In contrast, the non-collinear wave mixing technique shows the advantages of more flexibility in selecting the wave modes, frequencies, and propagating directions. The NRUS technique has been validated as particularly suitable to characterize the nonlinearity of granular materials such as concrete [111,112]. Time reversal is a promising NUT technique due to its advantage of being free of baseline signals [86,121].

3. NUT signal pre-processing and parameter analysis for damage characterization

3.1. NUT signal pre-processing and feature extraction

The nonlinear components in sensory wave signals induced by damage only account for a small proportion of the entire signals. Noise from the background or generated within the test equipment would interfere with identifying the nonlinear features. Signal pre-processing techniques can be used to de-noise and to extract nonlinear features. Several signal pre-processing techniques for extracting NUT features involve performing:

1. **Time domain statistics:** The easiest way to extract major features of time series data. In the context of NUT, important statistics include mean, standard deviation, peak-to-peak value, root mean square (RMS), kurtosis, skewness, crest factor, impulse factor, margin factor, etc. [129–131].
2. **Time–frequency transform:** The dispersive nature of Lamb waves causes the signals to distort and thus making the traditional spectrum analysis in the frequency domain not enough to extract specific wave packets. In contrast, the time–frequency (TF) transform is able to represent signals with a balance in time and frequency resolution.
3. **Sparse decomposition technique:** Sparse decomposition (SD) also called sparse representation aims to decompose a complex signal into components with over-complete dictionaries.

3.1.1. Time–frequency transform

Short-time Fourier transform (STFT) is the most basic TF transform technique. The time series signal is divided into overlapped segments by a sliding window, and the Fourier transform is performed on each segment. The STFT of the wave signal $x(t)$ can be expressed as [132]:

$$g_1(\omega,t)=\frac{1}{2\pi}\int_{-\infty}^{\infty}e^{-i\omega\tau}x(\tau)h(\tau-t)\mathrm{d}\tau \tag{4}$$

where $h(t)$ is the sliding window function, and w is the frequency. The energy spectrum of STFT calculated by $E_1(\omega,t)=\left|g_1(\omega,t)\right|^2$ is the well-known spectrogram.

Instead of using a fixed length window function, the wavelet transform (WT) uses a "mother" wavelet to perform signal transformation from time domain to TF domain. It has a higher frequency resolution and a lower time resolution in the low-frequency part; whereas a higher time resolution and a lower frequency resolution in the high-frequency part. The WT is given by:

$$g_2(a,b)=\frac{1}{\sqrt{a}}\int_{-\infty}^{\infty}x(t)\psi\left(\frac{t-b}{a}\right)\mathrm{d}t \tag{5}$$

where $a>0$ is the scale factor and b is the time-shift variable. a and b controls the shape and location of the wavelet, respectively. The energy spectrum of WT calculated by $E_2(a,b)=\left|g_2(a,b)\right|^2$ is called scalogram. Various "mother" wavelet (e.g. Gaussian, Morlet, Haar, Daubechies) $\phi(t)$ were designed to fit signals with different shape. A Gaussian wavelet is defined as :

$$\psi(t)=\frac{1}{\sqrt[4]{\pi}}\sqrt{\frac{\omega_0}{\gamma}}e^{-1/2(\omega_0 t/\gamma)^2+i\omega_0 t} \tag{6}$$

The Wigner–Ville distribution (WVD) represents the local energy distribution of signal and is defined as:

$$g_3(\omega,t)=\int_{-\infty}^{\infty}x\left(t+\frac{\tau}{2}\right)x^*\left(t-\frac{\tau}{2}\right)e^{-i\omega\tau}\mathrm{d}\tau \tag{7}$$

where $*$ denotes the complex conjugate.

In 1998, Huang [133] proposed a novel TF decomposition technique named Empirical Mode Decomposition (EMD). The EMD method decomposes signals to a set of intrinsic mode functions (IMFs) based on the local change characteristics of the signal itself. The EMD is established on the well-behaved Hilbert–Huang transform (HHT). The HHT is performed by calculating sum of IMFs as follows:

$$g_4(t)=\sum_{j=1}^{n}\alpha_j(t)\exp\left(\mathrm{i}\int\omega_j(t)\mathrm{d}t\right) \tag{8}$$

where $\alpha_j(t)$ is the envelope of the wave signal $x(t)$, n is the number of the IMFs, and $\omega_j(t)$ is the instantaneous frequency considered as the function of time. To obtain the IMFs, an algorithm called shifting process was proposed [133].

Niethammer et al. [132] investigated the effectiveness of four TF transform techniques to analyze Lamb waves. They found that the WVD is not capable of representing Lamb waves in the TF domain with a good resolution. Cantero-Chinchilla et al. [29] stated that the continuous wavelet transform (CWT) provides an overall better performance than HHT, WVD, and STFT on calculating ToF data of Lamb waves. Compared with Wavelet analysis, EMD does not require a base signal to be selected in advance. Sharma et al. [134] utilized the ensemble EMD to detect damages in coarse-grained austenitic stainless steels. The experiment showed that the SNR was increased by using ensemble EMD. Ara et al. [135] combined EMD and discrete wavelet transform (DWT) to extract non-redundant features. Although EMD has achieved good results in other fault diagnosis fields, it has a problem of mode confusion, which limits its application in ultrasonic signal pre-processing. To obtain a better decomposition result, the following properties are desirable:

1. The ultrasonic signal can be described by the bandwidth factor, center frequency, and initial phase of a narrow band signal modulated by the receivers tuned center frequency.
2. The ultrasonic signal acquired by the receiver is the convolution result of signal from the transmitter and from the specimen under inspection, which has the sparse property.
3. The probability density function of the ultrasonic signal have super-Gaussian property.

3.1.2. Sparse decomposition

The dispersive and multi-modal nature of Lamb waves cause the wave packets induced by damage to be mixed with other wave packets. In addition, the boundaries of the specimen introduce more wave propagation paths between actuator and receiver, which further complicates the wave packets. To this end, an advanced signal processing technique called SD is applied to decompose the dispersive Lamb

Table 3
Application of various NUT techniques for damage characterization in solid materials.

	Damage detection	Damage localization	Damage quantification
HH	Ti and steel crack [5,90]	Al breathing crack [122]	Ti crack [5]
Sub-harmonic	Al closed crack [93,97] Al disbond [98]	Al closed crack [94,95]	Al closed crack [94,95]
NWMS	Al fatigue [123] CFRP delamination [8]	Al fatigue [11]	Al fatigue [11,124]
Wave mixing	Al fatigue [77] Al plastic deformation [101] Steel crack [100] CFRP impact damage [106]	Steel crack orientation [125] CFRP delamination [126]	Steel crack [99,100] Steel corrosion [104] Al distributed cracks [102]
NRUS	Slate damage [110] Concrete thermal damage [111]	N/A	Steel corrosion [116] CFRP crack [115] Concrete thermal damage [112] Concrete ASR damage [113]
Time reversal	Al notch [88] Steel corrosion [119] Composite delamination [87] Composites damages [127]	Al closed crack [128] Composite damage [84,86]	Al closed crack [128] Pipe damage [120] Composite damage severity [78]

Al: Aluminum (alloy), Ti: Titanium (alloy), ASR: alkali–silica reaction.

waves. Mallat and Zhang [136] first proposed the SD method and introduced the matching pursuit (MP) algorithm. By establishing a custom dictionary to represent ultrasonic signals based on its narrow band and super-Gaussian properties, SD showed better results than TF transform methods.

Given an incident wave $u(t)$ propagates to position x, the resulting signal can be expressed as:

$$u(x,t) = \frac{1}{2\pi}\int_{-\infty}^{+\infty} F(\omega)e^{j\omega t}e^{-jkx}\,\mathrm{d}\omega \tag{9}$$

Considering the dispersive effects and multi-modal nature of Lamb wave, the received signals consists of multiple wave packets that can be given as [137]:

$$s_0(t) = \sum_m \frac{A_m}{2\pi}\int_{-\infty}^{+\infty} F(\omega)e^{j(\omega t - kx_m)}d\omega = \sum_m A_m u\left(x_m, t\right) \tag{10}$$

where x_m is the propagation distance of mth wave packet, and A_m is the corresponding amplitude.

Suppose that there are M wave packets in the received signals, and each wave packet is of length N. The received signal can be expressed as:

$$s_0(t) = \sum_{m=1}^{M}\sum_{n=1}^{N}\mathbf{u}_{mn}A_{mn} \tag{11}$$

where $\mathbf{u}_m$ denotes mth wave packet, and $\mathbf{u}_n$ denotes the sum of all wave packets at distance x_n. A_{mn} is the corresponding amplitude. From Eq. (9), the signal $\mathbf{u}_n$ at distance x_n can be written as:

$$\mathbf{u}_n = u\left(x_n, t\right) = \frac{1}{2\pi}\int_{-\infty}^{+\infty} F(\omega)e^{j\omega t}e^{-jkx_n}d\omega \tag{12}$$

Therefore, the over-complete dictionary composed of linear combination of $\mathbf{u}_n$ is given as:

$$\mathbf{U} = \left[\mathbf{u}_0, \mathbf{u}_2, \ldots, \mathbf{u}_n, \ldots \mathbf{u}_{N-1}\right]\mathbf{D}^{-1} \tag{13}$$

where $\mathbf{D}^{-1}$ is a diagonal matrix normalizing the dictionary to unit 2-norm. The dictionary is of the dimension of $M \times N$. The received wave signals can be represented by:

$$\mathbf{s}_0 = \mathbf{U}\mathbf{a} \tag{14}$$

where $\mathbf{a}$ is the amplitude factor matrix, and most of the factors are zeros because of the number of the wave packets is far less than the length of the received signals, making the sparsity of the wave signals.

Considering noise exiting $\mathbf{w}$ in the received signals

$$\mathbf{s}_0 = \mathbf{U}\mathbf{a} + \mathbf{w} \tag{15}$$

To obtain the amplitude factor matrix $\mathbf{a}$, the problem is converted to pursuit de-noising problem, which corresponds to an optimization problem [137]:

$$\arg\min_{\mathbf{a}}\|\mathbf{a}\|_1 \text{ subject to } \|\mathbf{s}_0 - \mathbf{U}\mathbf{a}\|_2^2 \leqslant \sigma^2 \tag{16}$$

Florian et al. [138] applied the SD technique for damage detection using NUT. The experiment showed that SD can extract useful ultrasonic signals from noisy data. Eybpoosh et al. [139] proposed an unsupervised feature extraction method for online damage detection in a pipeline. A dataset was established representing undamaged pipes by SD. The proposed method was validated by detecting various damages and structural abnormalities. Recently, SD has been combined with Bayesian inference as the sparse Bayesian learning (SBL) to accurately estimate the parameters of wave signals, which helps to solve the damage localization problem.

3.2. Damage index-based parameter analysis

Damage characterization requires further parameter analysis after applying signal pre-processing to the raw wave signals. Generally, a conventional way is to build a DI according to nonlinear mechanisms to characterize damages. Much literature characterizes DI in the time domain, frequency domain, and TF domain. In addition to the time statistics mentioned in Section 3.1, the DI construction methods can be divided into two directions:

New harmonics generation DI. New frequency harmonics are generated in HH, sub-harmonic, NWMS, and wave mixing testing scenarios with the presence of damage. A natural way of building DI is to measure the generated harmonics or quantify the ratio of them to the incident wave signals. For example, in the HH testing scenario, the nonlinearity parameter β is defined as:

$$\beta = \frac{8}{k^2 X}\frac{A_2}{A_1^2} \tag{17}$$

where k is the wavenumber and X is the wave propagation distance. A_1 and A_2 are absolute amplitudes of fundamental and second harmonic frequencies, respectively. The β parameter can be revised according to the different experimental configurations. Lim et al. [17] proposed the

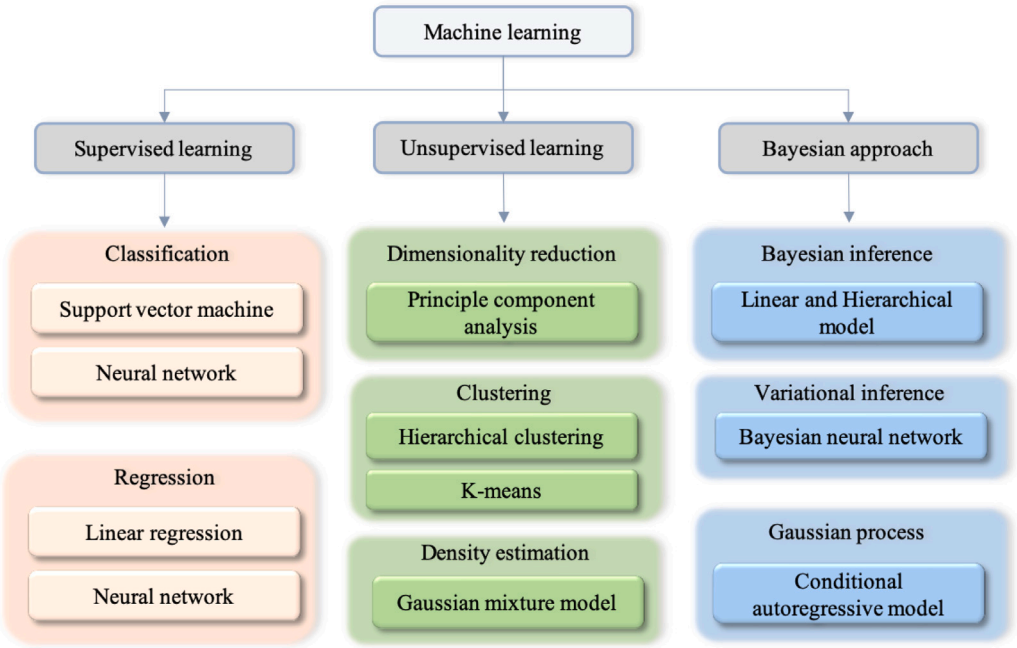

Fig. 12. Taxonomy of ML methods and representative algorithms.

cumulative β parameter to evaluate the nonlinearity when using Lamb waves. More variants of DI based on the β parameters can be found in [82].

Difference-based DI. Since many NUT techniques rely on measuring the difference between the testing signals with the baseline signals, various difference-based DIs have been proposed. A common way is to calculate the correlation coefficients of the testing signal and the baseline signal and the Pearson correlation coefficient is one of the most popular [140,141]. More advanced difference-based features can be found in [142–144]. Some DIs consider the whole spectral change of the wave signal in the frequency domain since the presence of damage may alter the frequency or resonance distribution such as the resonance shift when using the NRUS technique. Qing et al. [145] proposed a DI to measure the difference of frequency response of testing signals and baseline signals as:

$$\mathrm{DI} = \left| 1 - \frac{f_d^T f_d}{f_b^T f_b} \right| \tag{18}$$

where f_b and f_d are the spectral frequency response of baseline signal and testing signal, respectively. Gangadharan et al. [88] proposed to compare the WT coefficients difference of baseline and testing signals instead of spectral response to indicate damage presence.

Time reversal techniques rely on comparing the reconstructed signal with the incident wave signal to assess the nonlinearity of the specimen. Sohn et al. [87] proposed a DI defined as:

$$\mathrm{DI} = 1 - \sqrt{\left\{ \int x(t)y(t)dt \right\}^2 / \left\{ \int x(t)^2 dt \int y(t)^2 dt \right\}} \tag{19}$$

where $x(t)$ and $y(t)$ are the input signal and reconstructed wave signal, respectively. The proposed DI considers the attenuation effects, where a linear attenuation will not change the value of the DI.

3.3. Machine learning for damage characterization

With the rapid development of computing technology, ML methods have been widely explored in the fields of classification [146] and pattern recognition [147,148]. ML methods are capable of handling complex and multidimensional feature space to find latent nonlinear evidence of damage presence. Basically, ML methods can be categorized into supervised learning and unsupervised learning. In supervised learning, the objective is to build a predictive model from inputs to outputs of the labeled training data. Supervised learning tasks can be further classified into classification and regression. A classification model outputs categorical prediction and a regression model outputs continuous prediction. SVM and ANN are two well-established algorithms for classification; whereas, linear and logical regression are two examples of regression algorithms.

In contrast, in unsupervised learning, the data are not labeled. The unsupervised learning method aims at finding the internal structures of sub-dataset and distinguish them into several groups. Clustering, density estimation, and dimensionality reduction are the three main types of unsupervised learning algorithms. Clustering algorithms divide data into different clusters by evaluating the similarity of data, such as calculating the distance between data. Dimensionality reduction algorithms are often used as feature selection methods to project data into a lower-dimensional space. Density estimation algorithms assume data are random samples from a probability density function and strive to find this distribution. Apart from supervised learning and unsupervised learning, the Bayesian approach is considered the third paradigm of ML methods in this paper. Fig. 12 displays the categorization of main ML algorithms.

3.3.1. Supervised learning

Support vector machine. SVM realizes classification by finding a decision boundary hyperplane to separate data. Following the maximum margin principle, SVM uses a kernel function to realize the infinite-dimensional feature mappings. By adding a nonlinear kernel, such as polynomial or radial basis function, SVM separates instances that are nonlinear, making it suitable for classifying NUT data.

Given the training dataset $\mathbf{X} = \left[\mathbf{x}_1, \ldots, \mathbf{x}_M\right]^{\mathrm{T}} \in \mathbf{R}^{M \times N}$, where $\mathbf{X}$ includes M instances and each instance includes N features. $\mathbf{y} = \left[y_1, \ldots, y_M\right] \in \mathbf{R}^M$, where $\mathbf{y}$ is the label vector of M instances. SVM model aims to find the hyperplane to separate the instances. The target hyperplane is defined as:

$$f(\mathbf{X}) = \mathbf{w}^{\mathrm{T}}\mathbf{X} + b = 0 \tag{20}$$

where $\mathbf{w}$ and b are the weights and bias. In a binary classification task, two hyperplanes H_1 and H_2 outline the positive class and negative

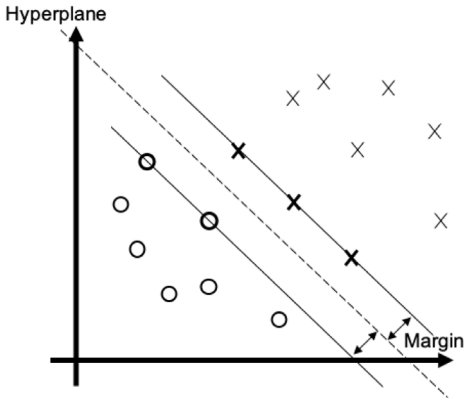

Fig. 13. Illustration of separating hyperplane for two-dimensional data.

class as shown in Fig. 13. The margin of the target hyperplane d_M, is defined as the distance between H_1 and H_2. Thus, the problem is converted to maximize the margin $d_M = 2/\|\mathbf{w}\|$. Since $2/\|\mathbf{w}\| = \frac{1}{2}\|\mathbf{w}\|_2^2$, the optimization objective can be written as [149]:.

$$\begin{aligned} &\min_{\mathbf{w},b} \quad \tfrac{1}{2}\|\mathbf{w}\|_2^2, \\ &\text{subject to} \quad y_i\left(\mathbf{w}^{\mathrm{T}}\mathbf{x}_i + b\right) \geq 1, \quad i = 1, 2, \ldots, M \end{aligned} \tag{21}$$

A binary SVM classifier can be used to detect damage. Agarwal and Mitra [27] built an SVM model following an MP step, which aims to reduce the noise in the Lamb wave signals. The experiments showed that the SVM model outperforms the ANN classifier model. Virupakshappa and Oruklu [150] proposed to use a split spectrum processing technique to decompose A-scan data and feed the reconstructed time-domain signal into an SVM model to detect holes in a steel block, where the damage detection accuracy can reach up to 98%.

To apply SVM in multi-class classification, several strategies have been proposed, such as one-again-all [151] and binary decision tree [152]. Das et al. [153] applied the one-class SVM to detect delamination in composites, where using time-domain features is more efficient compared to TF features for identifying delamination. Sun et al. [154] exploited the least squares support vector machine (LS-SVM) to boost the convergence, and genetic algorithm (GA) to find an optimized model. The prediction from their LS-SVM model showed good agreement with the experimental data to quantify fatigue crack in an aluminum plate. Zhang et al. [155] comprehensively studied the effectiveness of using SVM to identify damage severity and orientation. The grid searching method was used to find the optimal parameters of the SVM model. The SVM damage characterization model was applied to a diverse damage dataset, where 17 different damages with various kinds of types, sizes, and orientations were included. The results showed that using wavelet coefficients as input of the SVM model can reach a total accuracy of up to 95% when the noise level is below 100 dB.

Artificial neural networks. ANN is widely employed in computer science for its capability in learning underlying systematic features. Seeing the great success of ANN in computer vision, recommendation systems, and natural language processing, etc. Many researchers have applied the ANN to characterize damage using NUT. Fig. 14 is an illustration of a fully-connected neural network (FCNN) with one input layer, three hidden layers, and an output layer. Layers, which are composed of neurons are referred to as a set of functions. Each neuron has its own weight w and bias b. Given the training dataset $\mathbf{X} = \left[\mathbf{x}_1, \ldots, \mathbf{x}_M\right]^{\mathrm{T}} \in \mathbf{R}^{M\times N}$, $\mathbf{Y} = \left[\mathbf{y}_1, \ldots, \mathbf{y}_M\right] \in \mathbf{R}^{L\times M}$. The input of neurons in layer h is calculated with predecessor neurons in layer $h-1$. The output of FCNN is updated by the neurons in the last hidden layer H [156]

$$\hat{y}_j = \sigma^{\mathrm{out}}\left(\sum_{i=1}^{n_H} w_{ij}^{\mathrm{out}} \cdot x_i^H + b_j^{\mathrm{out}}\right), \quad j = 1, 2, \ldots, L, \tag{22}$$

where $\hat{y}_j$ is the output of jth neuron, σ^{out} is the activation function of the output layer, n_H is the neuron number of Hth layer, w_{ij}^{out} is the weight between jth neuron in output layer and ith neuron in the previous layer, x_i^H is the output of ith neuron in H layer and b_j^{out} is the bias of jth neuron in output layer. Activation function is a type of predefined function, such as sigmoid function, softmax function, and rectified linear units. The function used to calculate the error between prediction and the given label in the dataset is called a loss function. Using a quadratic loss function, the optimization objective of FCNN aims to minimize:

$$\min_{\mathbf{W},\mathbf{B}} L = \frac{1}{2}\sum_{j=1}^{L}\left[\left(\mathbf{y}_i\right)_j - \left(\hat{\mathbf{y}}_i\right)_j\right]^2 \tag{23}$$

where $\mathbf{W}$ and $\mathbf{B}$ is the matrix of weight and bias, respectively. The back propagation [157] and gradient descent algorithm are used to update the weights and biases as follows.

$$\mathbf{W}^{\mathbf{new}} = \mathbf{W}^{\mathbf{old}} - \eta \cdot \frac{\partial L}{\partial w}, \quad \mathbf{B}^{\mathbf{new}} = \mathbf{B}^{\mathbf{old}} - \eta \cdot \frac{\partial L}{\partial b}, \tag{24}$$

where η is the learning rate. The extracted feature of ultrasonic wave signal in time domain and frequency domain is fed into the input layer such that the output layer can predicted the materials status, i.e. undamaged or damaged.

To obtain a good ANN-based damage detector, reasonable hand-crafted features are required. Thus most of the researches using ANN to detect damage focuses on investigating the model performance with different feature extraction methods. TF transform methods were firstly investigated as the feature extraction techniques for ANN inputs. Legendre et al. [158] used the wavelet coefficients from DWT of Lamb waves signals as the input to an ANN model with three layers. The classification accuracy of their ANN model was 90% to detect porosity in welds. Simone et al. [159] compared DWT, discrete Gabor transform (DGT), and clustered DWT as the pre-processing techniques to provide input to the ANN. Experimental results demonstrated that the clustered DWT pre-processing had better overall performance than DWT and DGT to detect damage on welds. A more direct way to build damage features is to evaluate the difference between testing signals and baseline signals in the time domain. Su and Ye [160,161] proposed to use the down-sampled wave signals as the input of the ANN model. The experiments conducted on a carbon fiber/epoxy (CF/EP) plate-like structure validated that the ANN model can identify artificial cracks. However, the length of cracks exceeds 10 mm. Therefore, the effectiveness of using the proposed method to detect small cracks was not validated. Nazarko and Ziemianski [162] proposed an auto-associate neural network (AsNN) model to identify the damage. The idea of AsNN is to learn the input data distribution, and the output vector of the model is supposed to be identical to the input vector. It measures the distance of the output vector and input vector to evaluate whether there is a presence of damage. The proposed methods can identify damage in different locations in aluminum and composite specimens. However, the effectiveness of the proposed method was not validated on complex structures. Dworakowski et al. [143] used four normalized squared error-based and Pearson cross-correlation-based DIs as the input of the ANN model to detect damage. In addition, to increase the reliability of the damage detector, they employed an ensemble algorithm, where four basic ANN models were included. The test on industrial specimens validated the ensemble models provides a better result than the single ANN model.

For the damage localization problem, Sbarufatti et al. [144] defined DIs as several dominant eigenvalues of the data matrix composed of wave signals collected from multiple actuator–receiver paths. The DIs were used as inputs of the ANN model to predict the damage location and length. The crack length used in the experiment ranged from 5 mm to 70 mm and the average estimation error from the ANN model is about 2.3 mm. The performance of the ANN model in the damage location estimation is significantly affected by the length of the

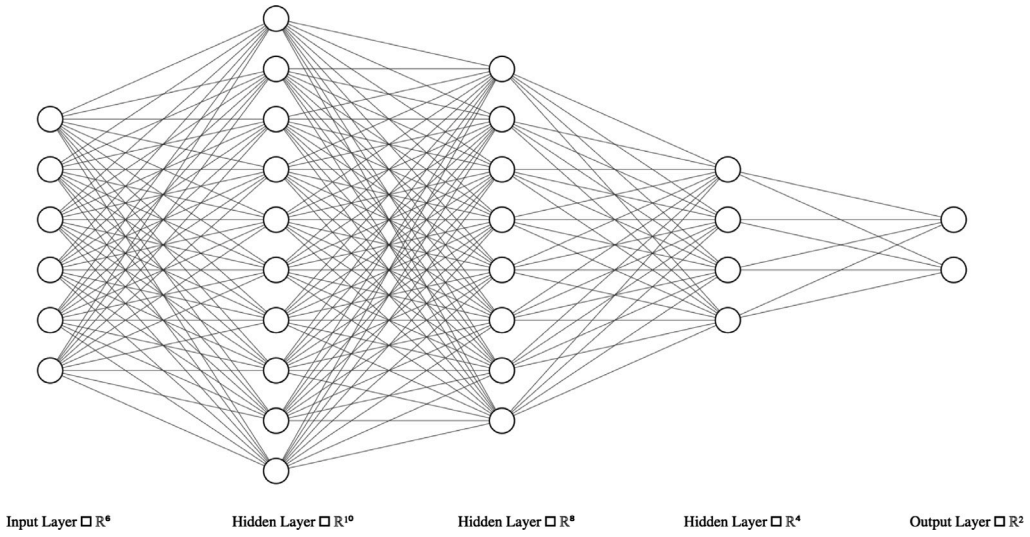

Fig. 14. Architecture of a fully-connected neural network with 5 layers.

crack. When the length of the crack is 5 mm and 10 mm, the average estimation error of the damage location coordinates can reach 30 mm. De Fenza et al. [163] proposed to use DI defined as the signal difference between damaged and undamaged specimen in the frequency domain as the input of the ANN model. The proposed ANN model was able to identify the damage location region, where a plate-like structure was evenly divided into 16 regions. However, the proposed model was not able to provide an accurate coordinate of the damage location. Feng et al. [39] used the ToF data from three wave propagation paths as the input of an ANN model to locate the damage. The average error is 2.8 mm using the ANN model to estimate the coordinates of a 6 mm diameter circular damage. The limitation of this algorithm is that it requires a large volume ToF-location pairs data to train the model.

The ANN-based regression model can be used in damage quantification problem. Lim and Sohn [17,26] used the NWMS technique to collect data for an ANN model for fatigue crack quantification and prognosis. The thickness of the specimen, loading cycles of testing, and the β parameters were used as inputs to the ANN model. The maximum error of the ANN model prediction on the crack length and remaining useful life was 1.35 mm and 2000 cycles, respectively. However, the proposed input configuration is only validated on an aluminum plate, the generalization ability of the model on complex structure and composite materials needs to be verified.

3.3.2. Convolutional neural networks

CNN was developed from ANN, where a hierarchical structure was employed to capture high-level features and to learn more complex mapping between input and output. The development of CNN boosts the application of computer vision and natural language processing, and also provide a promising solution to the damage characterization using NUT. Compared with the ANN, CNN has the following characteristics:

1. **Free of handcrafted features:** Unlike ANN, CNN dose not require handcrafted features and it mimics the feature extraction process by feeding raw data directly and stacking neural network layers. Meanwhile, different CNN algorithms have been developed to process 2D images and sequence data.
2. **nonlinearity:** Layers such as convolutional and regularities such as batch normalization and dropout allow CNN to capture nonlinearity and reduce overfitting [164].
3. **Large volume data:** CNN requires a large volume data for training to obtain a good model performance. However, this could be a challenge to apply CNN into NDT&E application scenarios since a large amount of data are difficult to obtain.

2D convolutional neural networks. CNN was applied to computer vision tasks in late 1980 and it has been the most widely used ML algorithm after decades of development. A basic CNN structure consists of convolutional layers, pooling layers, and fully connected layers. Fig. 15 illustrates the CNN structure proposed by LeCuN [165], which was well known as LeNet. The input of the LeNet is supposed to be 2D, such as images. The convolutional layer works as a filter, where the input from the previous layer is convolved with a kernel function. The kernel function is defined as a set of weights and scales the images by locally multiplying its elements with the elements of the corresponding receptive field of input. The output of the convolutional layer and pooling layer is called feature-map. Given the kernel $k^c \in \mathbf{R}^{U\times V}$ and the input matrix $\mathbf{X}^{c-1} \in \mathbf{R}^{M\times N}$ from the previous $c-1$ layer, the cth layer feature-map can be expressed as follow:

$$\begin{aligned} \mathbf{X}_i^c &= f_c\left(\mathbf{X}_i^{c-1} * \boldsymbol{k}^c + \boldsymbol{b}^c\right) \in \mathbf{R}^{(M-V+1)\times(N-U+1)}, \quad c = 2, 3, \ldots \\ \left(\mathbf{X}_i^{c-1} * \boldsymbol{k}^c\right)_{j,k} &= \sum_{m=1}^{M}\sum_{u=1}^{U}\sum_{v=1}^{V} x_{(i),j+u-1,k+v-1,m}^{c-1} \cdot k_{u,v}^c \end{aligned} \tag{25}$$

where f_c is the activation function of the $c$the layer. The CNN has the weight sharing characteristics that feature-map can be obtained by sliding the kernel with same weights. The pooling layers also known as down-sampling layer is to extract information of the receptive field following a specific operation. For example, the max-pooling operation represents a receptive field by its maximum value. Other types of pooling operation such as average, overlapping, etc. are also used in CNN [166,167]. The pooling operation downsizes the images, which not only can help reduce the complexity of the model but also contribute to avoid overfitting [168]. The last pooling layer is followed by fully-connected layers, which are similar to that in ANN.

Following the LeNet, researchers have extensively developed the CNN with many novel architectures. The main thrust in CNN innovation has been made in depth and width exploration, feature-map exploitation, computation boosting, new block and link design, and attention mechanism [168]. The most representative ones are AlexNet [169], VGG [170], and ResNet [167]. However, these CNNs also referred to as 2DCNNs are designed to process 2D data, and unable to process 1D signals, such as ultrasonic wave signals. To this end, signal pre-processing is required before feeding data to a 2DCNN model.

A natural way is to use TF transform to convert 1D wave signals to 2D images. Meng [171] utilized wavelet packet decomposition to transform a wave signal with 512 samples into a 2D feature matrix with dimensions 32×16. The transformed feature matrix was then fed into a

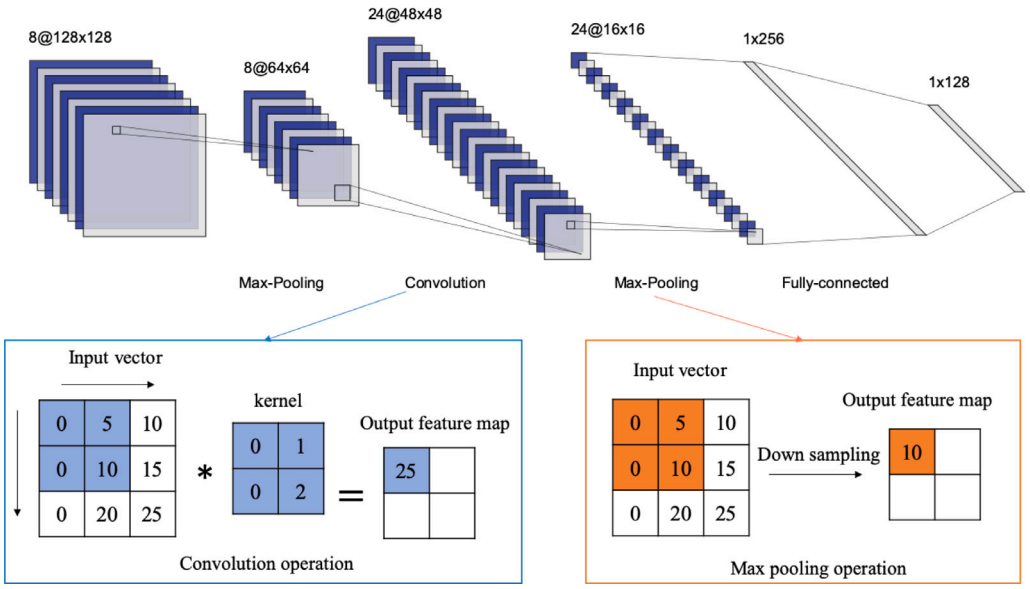

Fig. 15. Architecture of LeNet and illustration of convolution operation and pooling operation.

CNN model with two convolutional layers and two pooling layers. The author constructed handcrafted DIs including statistics parameters of wavelet coefficients and Shannon entropy. An experiment on a CFRP specimen showed that the CNN classifier was able to detect delamination damage with an accuracy rate over 97%, which outperforms the handcrafted DIs. Melville et al. [172] also used the WT as the pre-processing technique for the CNN model. They compared the damage detection performance of CNN and SVM, and the experiment on an aluminum plate showed CNN is able to detect 2 g mass with 99% accuracy compared to the SVM with 62% accuracy. Liu and Zhang [173] adopted the VGG architecture in detecting notch damage on the aluminum plate. In their test, the VGG model achieved an accuracy of more than 98% compared to the accuracy of 64% when using a simple ANN model.

For the damage localization and quantification problem, Su et al. [174] reshaped the 900 frequency points of the wave signals spectrum into 30 × 30 feature matrix as the input of a CNN model with two convolutional layers and two pooling layers. Features from three actuator–receiver paths were fed into the CNN model to locate a mass block and identify the size of the mass. Although the CNN model was able to identify and distinguish the size of the mass, it can only provide the region of the mass on the plate instead of accurate coordinates.

1D convolutional neural networks. Although pre-processing techniques can be used to convert the 1D wave signals to 2D images, the advantage of CNN exploiting the data characteristics without feature extraction process is lost. To this end, the 1DCNN was developed to incorporate 1D signals. Compared with 2DCNN, the convolutional layer and pooling operation in 1DCNN is conducted in 1D. The fully-connected layers are identical to those in 2DCNN. Innovation in applying 1DCNN to analyze 1D signals lies in input data manipulation, processing neural units, and architecture construction.

In a multi-class damage identification task, Munir et al. [30] built a basic 1DCNN model, which consists of two convolution layers, one pooling layer, and two fully-connected layers as shown in Fig. 16. The raw 1D wave signal was fed into the CNN model directly as an input and a 1D convolution operation was then applied. The authors also built a deep FCNN model with three hidden layers and three dropout layers. They simulated crack, lack of fusion, lack of penetration, porosity, and slag inclusions damages on a welded specimen under five noise levels ranged from SNR 5 dB to SNR 20 dB. Overall, 1DCNN provided better damage detection performance than deep ANN, and the greater the noise, the higher the accuracy of CNN over ANN. When SNR is 5 dB, the accuracy of CNN exceeded deep ANN 4.59%, 10.80%, and 15.45% for cracks, lack of penetration, and slag damage, respectively.

Xu et al. [31] also applied 1DCNN for damage detection and proposed to fuse wave signal features from multiple actuator–receiver paths to increase robustness. As shown in Fig. 17, they first extracted seven features including time domain statistics and spectrum based DIs from each path, and sequentially concatenate all DIs from different paths as input. They applied the proposed model on various sizes of cracks on an attachment lug specimen and conducted comparison experiments. Three configurations were tested: (1) CNN model with multiple paths features as input, (2) CNN model with single path feature as input, and (3) an ANN model with features from multiple paths as input. The results showed that the proposed CNN with features from multiple paths as input gave the best performance. However, they did not investigate the CNN performance using raw multiple wave signals as input.

It was reported that multi-headed CNN, which consists of multiple parallel CNN models, can learn high-level features more efficiently [175]. Rai and Mitra [176] introduced multi-headed CNN to detect damage in metallic plates. In their model, raw 1D wave signal was fed into two parallel CNN models and the output of these sub-models was flattened followed by fully-connected layers. The proposed model was applied to notch damage detection on an aluminum plate-like structure. Compared to 2DCNN, the multi-headed CNN requires less computation time without any decrease in accuracy. However, the structure of the testing specimen was simple and the damage was designed on the direct propagation path between actuator and sensor, which is easy to identify. Zhang et al. [177] further developed the multi-headed CNN by applying 2D convolutional operation in sub-models. They also proposed a time-varying DI defined as the energy ratio of the current signal to the baseline signal. To allow time information in the DI, the wave signal was split into overlapped segments and the DI was calculated in each segment. With time information, the DI is able to identify the damage location. The DIs extracted from multiple actuator–receiver paths were fed into the multi-headed CNN model. Fig. 18 illustrates the architecture of the proposed 1DCNN model. The proposed model can provide coordinates of the damage. The experiment on an aluminum plate showed that the proposed method can significantly outperform the ellipse-based damage localization method.

Ince et al. [178] proposed a novel 1DCNN architecture for fault detection, where the pooling was assembled to a convolutional layer

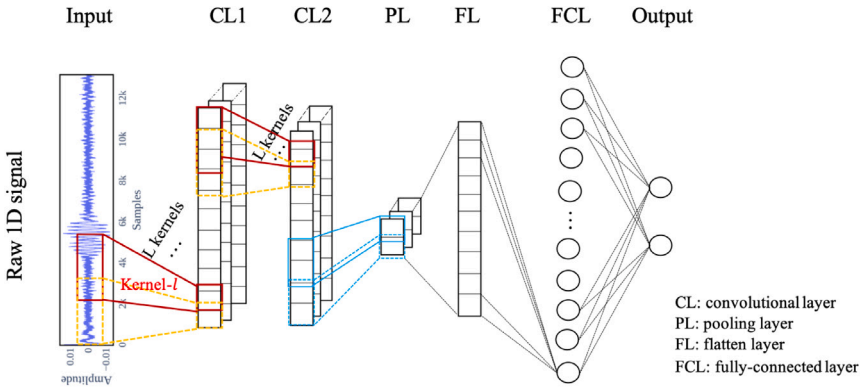

Fig. 16. Architecture of 1DCNN with basic convolutional, pooling, and fully-connected layer.

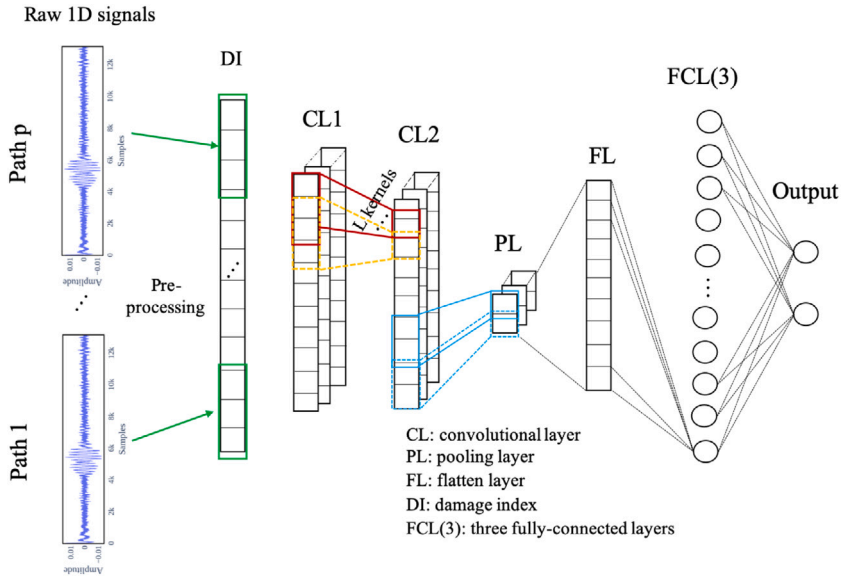

Fig. 17. Architecture of 1DCNN with multiple 1D signals used as input.

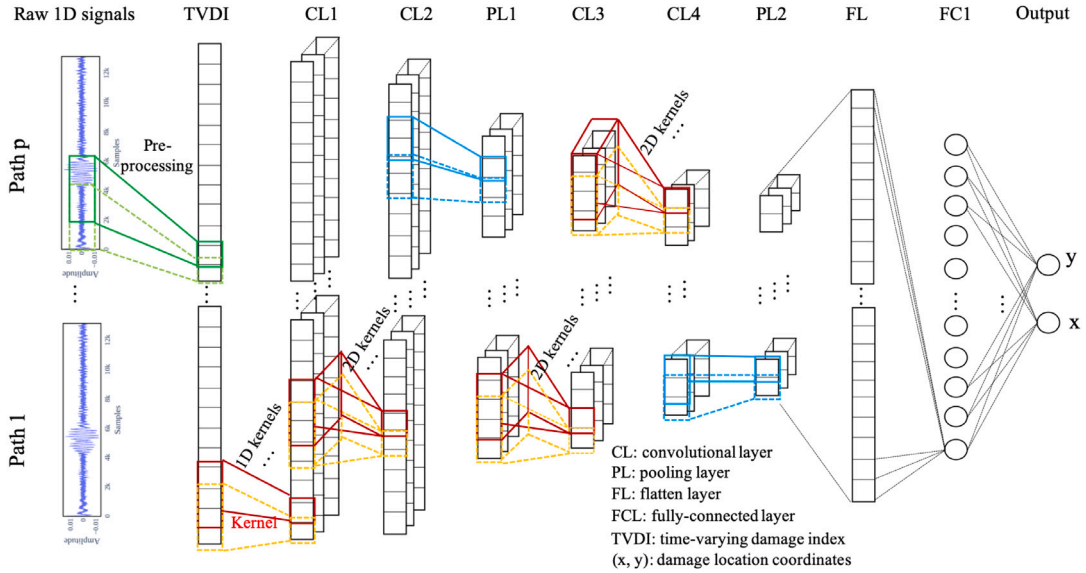

Fig. 18. Architecture of the multi-headed 1DCNN for damage localization.

as an intermediate operation. Fig. 19 illustrates three consecutive CNN layers. A set of convolutions was performed on the outputs of the last layers and a summation was applied. Then, a down-sampling operation working as the pooling layer was applied. The output of this layer is feature-maps of the down-sampled data performed by multiple 1D kernels. The author applied the proposed 1DCNN algorithm to detect the fault in the motor and obtain a good result. Investigation of applying the 1DCNN to NUT-based damage characterization has not been performed.

3.3.3. Unsupervised learning

A major advantage of unsupervised learning is that it does not require labeled training data. Unsupervised learning aims to find the space distribution of the dataset, where a model is optimized to fit the input feature matrix.

Principal components analysis. Principal components analysis (PCA) is widely used to reduce the feature dimension [179]. The lower-dimension features dominating the majority of variance in the dataset are called principal components. The main idea of PCA is to transform the dataset into a new coordinate system through an orthogonal linear transformation, where the total data variance along the principal direction is maximized. Given the feature matrix $\mathbf{X}$, the principal components $\mathbf{P}$ can be obtained using singular value decomposition of $\mathbf{X}$:

$$\mathbf{X}^T\mathbf{X} = \mathbf{P}\Sigma^2\mathbf{P}^T \tag{26}$$

where $\mathbf{P} = \left[\mathbf{p}_1, \ldots, \mathbf{p}_N\right] \in \mathbf{R}^{N\times N}$ are the principal components, and $\Sigma^2 = \text{diag}\left(\left[\sigma_1^2, \ldots, \sigma_N^2\right]\right) \in \mathbf{Z}^{N\times N}$ are the square diagonal matrix with the variances of $\mathbf{X}$ along the principal components $\mathbf{P}$.

One of the well-known applications of PCA for NDT&E is for feature selection. Of various features extracted using time and frequency-domain techniques, the PCA method is used to decrease the noise level before employing further correlation analysis [180]. Miao et al. [181] combined the PCA and SVM methods for detecting crack using a pulse-echo setup. A total of 14 features including 9 in the time domain and 5 in the frequency domain were extracted. The PCA was first used to reduce the number of features to discriminate between damaged and undamaged specimens. The reduced features were then fed into the SVM-based classifier for crack detection.

GaussIan mixture models. In the experiment and industrial applications, uncertainties from the equipment, measurement, and time-varying ambient conditions can introduce errors in the sensor signal. These uncertainties would further corrupt the extracted features leading to large variances in the evaluation results. These features can be considered as random variables that follow a joint probability density function (PDF). To reduce the influence of these uncertainties, a plausible solution is to estimate the feature properties using a probabilistic model. Gaussian mixture model (GMM) assumes the features are sampled from a mixture of a finite number of Gaussian distributions with unknown weights. Given the dataset: $\mathbf{X} = [\mathbf{x}_1, \ldots, \mathbf{x}_m, \ldots, \mathbf{x}_M]^{\mathrm{T}} \in \mathbf{R}^{M\times N}$, where $\mathbf{x}_m$ includes N features. The PDF of GMM can be modeled as: [182]

$$F\left(\mathbf{x}_m|\mu, \mathbf{\Sigma}\right) = \sum_{k=1}^{K} w_k f_k\left(\mathbf{x}_m|\mu_k, \mathbf{\Sigma}_k\right) \tag{27}$$

where K is the number of Gaussian distributions, $\theta = \{w_k, \mu_k, \Sigma_k\}$ are the mixture weight, mean, and covariance of the $\mathbf{k}$th Gaussian component, respectively. The PDF of each Gaussian components is a N-dimensional multivariate Gaussian distribution with N features:

$$f_m\left(\mathbf{x}_m|\mu_k, \mathbf{\Sigma}_k\right) = \frac{1}{(2\pi)^{\frac{N}{2}}\left|\mathbf{\Sigma}_k\right|^{\frac{1}{2}}} \mathrm{e}^{-\frac{1}{2}(\mathbf{x}_m-\mu_k)^T\mathbf{\Sigma}_k^{-1}(\mathbf{x}_m-\mu_k)} \tag{28}$$

The problem of finding the optimal parameter K is computationally difficult. Hence, an iterative method called expectation–maximization algorithm (EM) is introduced to find the maximum likelihood estimates of the parameters. In every EM iteration, there is an E-step, which creates an expectation function of the log-likelihood given the currently estimated parameters of the dataset, and a M-step, which updates the parameter to maximize the expectation function created in the E-step. The log-likelihood $L\theta$ of the dataset X is subject to:

$$L(\theta) = \sum_{m=1}^{M} \log F\left(\mathbf{x}_m|\theta\right) \tag{29}$$

According to Bayes' theorem, the posterior probability of $\mathbf{m}$th instance assigned to Gaussian component k in E-step is:

$$\phi_{km} = P\left(\mathbf{x}_m|\mu_k, \mathbf{\Sigma}_k\right) = \frac{w_k\mathbf{\Phi}_k\left(\mathbf{x}_m|\mu_k, \mathbf{\Sigma}_k\right)}{\sum_{j=1}^{K} w_j\mathbf{\Phi}_j\left(\mathbf{x}_m|\mu_j, \mathbf{\Sigma}_j\right)} \tag{30}$$

where $\phi_k = \sum_{m=1}^{M}\phi_{km}$, is the weighted number of instances clustered to centroid k. other variables are also not defined in the previous equation.

The M-step updates the parameters $\theta = \{w_k, \mu_k, \Sigma_k\}$ by:

$$\begin{aligned}
\hat{w}_k &= \frac{1}{M}\sum_{m=1}^{M}\phi_{km} \\
\hat{\mu}_k &= \frac{1}{\phi_k}\sum_{m=1}^{M}\phi_{km}\mathbf{x}_m \\
\hat{\Sigma}_k &= \frac{1}{\phi_k}\sum_{m=1}^{M}\phi_{km}\left(\mathbf{x}_m - \hat{\mu}_k\right)\left(\mathbf{x}_m - \hat{\mu}_k\right)^{\mathrm{T}}
\end{aligned} \tag{31}$$

The EM algorithm will be terminated when the variation of log-likelihood (calculated using Eq. (29)) is under a predefined threshold.

Qiu et al. [182] proposed an online GMM model to detect fatigue damage. Two parameters — the time domain cross-correlation coefficient and frequency amplitude difference between baseline signal and current signals were used for damage characterization. A reference GMM was trained using baseline signals off-line, and an online GMM is constructed by feeding the new monitoring signals. A queue sample set was considered to keep the feature sample compact. The Kullback–Leibler divergence was used to evaluate the difference between two GMMs, where divergence above a predefined threshold would indicate damages. Qiu et al. [183] further developed the GMM-based monitoring system to make it more robust and efficient by using density peaks clustering-based EM algorithms. Wang et al. [14] attempted to evaluate time-domain statistics including RMS, variance, skewness, and kurtosis as the parameters of a GMM model. The accuracy of detecting corrosion, impact hole, and crack damages in glass fiber reinforced composites are 88.10%, 80.95%, and 80.95%, respectively.

K-means. K-means is an unsupervised learning method for clustering similar data by learning data structures. Unlike GMM, K-means evaluates the dataset by calculating the distance between instances. The goal of K-means is to generate a finite number of clusters, where instances belong to a cluster with the nearest centroid. K-means is also an iterative algorithm and the implementation process can be expressed as follows:

1. Randomly assign k cluster centroid from the input dataset.
2. Calculate the distance between all instances with k centroid.
3. Assign instance to the nearest centroid.
4. Update the centroid of one cluster by calculating the mean of the instances within the cluster.
5. Repeat step (2) to (4) until the centroids no longer change.

K-means is also a computationally difficult problem and thus a variety of heuristic algorithms were developed as improvements. Among them, Lloyd's algorithm is the most widely used [184]. The distance metrics should be determined according to the characteristics of the dataset. A comparative study on the effects of Euclidean, Manhattan, and Minkowski distance on K-means clustering can be found in Ref. [185]. It should be noted that K-means is likely to converge to a local optimum, and thus repeated experiments are preferred to find the

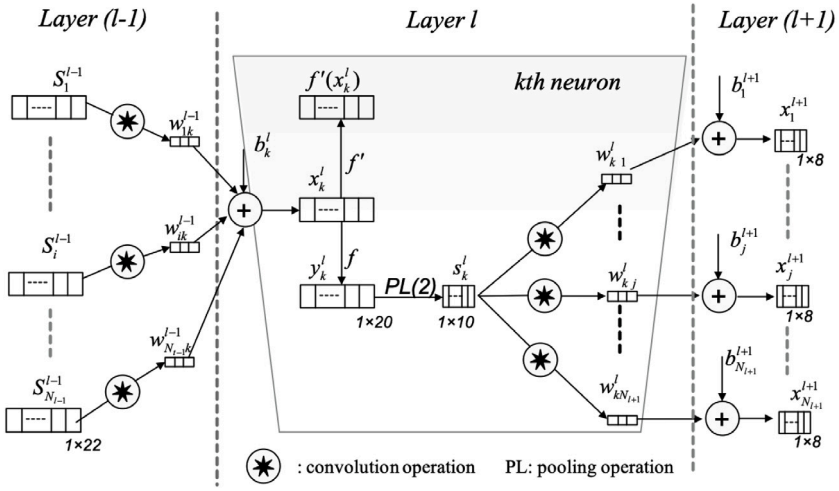

Fig. 19. Illustration of three consecutive layers in a novel CNN model.

best model. There is limited literature about using K-means to assess damage in materials using NUT. Bouzenad et al. [186] proposed to use K-means as a base clustering tool and applied the semi-unsupervised algorithm to determine the threshold of the appearance of damage. Four levels of damage severity were simulated by adding magnetic blocks to a pipe-like structure. The proposed K-means cluster was able to distinguish different levels of additive mass. However, K-means requires determining the number of k in the training process. In the industrial application scenarios, the k can be easily set as 2 when using K-means for the damage detection task. When comes to identifying the severity of the damage, it would be difficult to set an optimal k since the real damage conditions are much more complicated to categorize.

3.3.4. Bayesian approach

Bayes' theorem has been widely used in many ML methods, such as the GMM. It provides a simple framework for parameter inference, where prior knowledge is integrated. Expert knowledge is implemented to give a reasonable prior assumption. As more information from the dataset is fed into the model, the parameters can be updated to reduce uncertainties. Bayes' theorem can be expressed as.

$$p(\mathbf{y}|\mathbf{x}) = \frac{p(\mathbf{x}|\mathbf{y})p(\mathbf{y})}{p(\mathbf{x})} \tag{32}$$

where $\mathbf{x}$ and $\mathbf{y}$ are different events. In the context of a ML model, given the input $\mathbf{x}$ and output $\mathbf{y}$ with model parameters θ. The objective is to estimate θ to make the output approach the ground truth. The estimated θ conditioned on dataset can be obtained by:

$$p(\theta|\mathbf{x},\mathbf{y}) = \frac{p(\mathbf{y}|\mathbf{x},\theta)p(\theta|\mathbf{x})}{p(\mathbf{y}|\mathbf{x})} \tag{33}$$

where $p(\theta)$ is referred as prior distribution, $p(\mathbf{y}|\mathbf{x},\theta)$ and $p(\theta|\mathbf{x},\mathbf{y})$ are called likelihood and posterior, respectively. The conditioned probability of $p(\mathbf{y}|\mathbf{x})$ cannot be computed theoretically as the distribution function of dataset is usually unknown. However, it can be approximated by sampling using Markov chain Monte Carlo (MCMC) simulation. Literature [187] gives a detailed introduction to MCMC for ML application.

Bayesian approaches are capable to reduce uncertainties from measurement and time-varying ambient conditions, and thus make it possible to accurately estimate the parameters of the wave signals. In the damage localization problem, the most common idea to estimate the damage location is to calculate the ToF data of multiple wave propagation paths and then solve the elliptical equation. Another method called the reconstruction algorithm for probabilistic inspection of defects (RAPID) [188] predicts the damage location based on the correlation analysis between testing signals and baseline signals. When using elliptical methods, the accuracy of ToF data and uncertainties are two major factors in the estimation of damage location.

Uncertainties.

1. **Measurement uncertainty:** The measurement noise may deteriorate the accurate calculation of ToF.
2. **Mathematical uncertainty:** The elliptical equation is ill-conditioned and ill-posed. A small deviation in the ToF can result in much larger errors in the damage location.

Tof estimation errors.

1. **Dispersion effects:** Guided waves have dispersive and multimodal in nature, which may cause mode conversion and overlap in the received wave signals. Mode conversion and overlap would affect the calculation of ToF data.
2. **Heisenberg principle:** When TF transform is used to extract the wave packet scattered by damage, the Heisenberg principle would affect the accuracy of the ToF data estimation.

To address the challenges listed above, several methods have been proposed. Among them, the Bayesian inference approach and SBL were developed to improve the damage localization accuracy. Yan [28] established a Bayesian model using the ToF data to update the probability density function of damage location and wave group velocity. The MCMC was employed to sample the posterior distributions of these parameters. Numerical and experimental results showed that the proposed method was able to provide a more accurate estimation of the wave velocity and damage location compared to the ellipse method. Ng [189] extended the estimation parameters to include damage length, depth, and location. A hybrid particle swarm optimizer was used in the Bayesian model. The estimated damage length and depth errors are less than 2%. Fendzi et al. [190] further developed Yan's [28] work to make it applicable in the anisotropic materials. He and Ng used the Bayesian approach to identify multiple delamination [191] and cracks [192] in beams and found that A_0 mode is more sensitive for identifying small crack (1 mm) than S_0 mode. Researchers have applied the Bayesian inference to detect complex damage in aerospace composite structures [193]. To address the problem of unappropriated selection of TF transform methods in calculating the ToF, Cantero-Chinchilla et al. [29] proposed to build a probabilistic model to select the TF transform method automatically. Huo et al. [194] fuse the elliptical method and RAPID method based on the Bayesian inference approach. The proposed method outperformed the traditional elliptical method and the RAPID method. However, the author did not provide comparison results of proposed methods with other Bayesian approaches. In addition to damage localization, some researchers have used the Bayesian methods for damage quantification [13,25] and for the remaining useful life prediction [195].

Instead of using the TF transform to extract wave packets, SBL decomposes the received wave signals into individual wave packets and then calculates the ToF of the wave packet induced by damages. In an SBL model, the elliptical equation was linearized using Taylor expansion, and l_0, l_1 minimization have been introduced for regularization purposes. Wu et al. [196] studied the availability of using SBL to extract wave packets from noisy signals in a pulse-echo setup. When the SNR is -8 dB, the relative error of time-delay estimation was under 1%. Xu et al. [197,198] utilized SBL to estimate traveling distance and then applied it to the damage localization problem. The experiment on a 500 × 500 mm plate-like structure shows that the proposed method can separate two overlapped wave packets with errors around 5 mm. One of the most recent works of using SBL to locate damages was studied by Zhao [199]. The author proposed to decompose signals with wave packets through SBL, where an over-complete dispersive wave signal dictionary was built, along with an over-complete distance dictionary for locating damages. An adaptive sampling strategy was proposed to map the propagation distance to the damage location regions. The relative errors of estimating the distances are under 2%.

Although unsupervised learning does not require labeling data for training, its application in damage characterization using NUT is still limited. The main reason is that the data challenge in the context of NUT is the scarcity of experimental and industrial large volume data instead of massive labeling work. Most researchers use unsupervised learning algorithms as feature selection techniques for further analysis. Tripathi et al. [200] conducted a comparison experiment on several classifiers with or without using PCA. The experimental results showed that PCA can reduce data dimension while retaining prominent features. In contrast, the use of supervised learning boosts the development of parameter analysis of NUT data. SVM and ANN have been validated in the damage detection task with high accuracy. However, ANN and SVM require reasonable handcrafted features as input to obtain a good performance. A promising solution to address this problem is to use feature selection methods such as PCA and GA. CNN is demonstrating great potential in solving damage detection, localization, and quantification problem without requiring handcrafted features. And the Bayesian approaches show effectiveness in estimating damage location with accurate coordinates due to their ability to reduce uncertainties. Table 4 summarizes the pros and cons of main ML algorithms for different damage characterization tasks.

4. Future directions

In this section, current challenges and suggestions for future research directions of ML-enriched NUT for damage characterization are discussed.

Data augmentation. To build a high-performance ML model for damage characterization, a large-scale dataset is required. However, the dataset from high-value structures such as aircraft is difficult to obtain, thus making the data augmentation a necessary step in the process of building an ML model. Currently, researchers perform data augmentation in two ways: (1) Build a high-fidelity FEM model to generate simulation data to compensate for the limited and expensive experimental results. (2) Enlarge the experimental dataset by adding noise or performing data manipulation. Munir et al. [30] used the time shifting technique to augment the damage data for training a CNN model. Zhang et al. [177] realized data augmentation by rotating the testing plate while retaining the position of the transducer. Rai et al. [176] added multiple levels of Gaussian noise to the raw signal to generate more data for training.

Complex damage characterization. Although progress has been made in using ML for damage characterization, a lot of efforts are needed in the complex damage characterization scenarios:

1. **Complex structures:** For the damage detection task, most existing researches only validated the effectiveness of using ML algorithms such as SVM and CNN on plate-like structures. Research on complex structures is still limited. A complex structure can complicate the wave propagation and increase the difficulty to extract effective handcrafted features. Therefore, the use of deep learning such as CNN in complex structure inspection appears promising.
2. **Micro-damage detection:** The biggest advantage of NUT is the sensitivity to the micro-damage and this has been validated in the research of direct problem. However, most published work only validated the effectiveness of using ML for damage detection where the size of the damage is larger than 2 mm [155]. More experimental research to validate the effectiveness of using ML to detect microscopic damages is needed.
3. **Multi damage localization:** Although the Bayesian approach can provide accurate coordinates of damage location, it has the challenge of locating multiple damages. besides, the Bayesian approach-based damage localization methods rely on the accurate estimation of ToF data. However, the increase in the number of damage complicates the wave propagation path and increases the number of new wave packets in the sensory signal, which causes difficulty in extracting the proper damage-induced wave packet. Another promising way to locate multiple damages is to use CNN to learn the multi-damage distribution through large-scale data mining operations. However, in addition to the data challenge, CNN-based models suffer the problem of difficulty in interpreting the results. To address this problem, the visualization technology is expected to figure out what the convolutional layers learn from the input.
4. **Remaining useful life prediction:** For the damage quantification task, most work can only identify different sizes of damages instead of providing size prediction [201]. Lim [17] validated the effectiveness of using the ANN model to predict the crack length and remaining useful life on aluminum plate-like structures. However, investigations on other types of materials and more complex structures have not been carried out due to the lacking of run-to-fail data for training. One advancement in ML for addressing this data challenge is transfer learning [156,202], which aims to transfer knowledge from one task to another.

Baseline-free methods. Most NUT methods require baseline signals from a pristine (damage-free) specimen to provide a reference for testing signals to identify changes induced by damage. However, these methods may be unreliable in the real industrial application since baseline signals may be unavailable and would be ineffective when the ambient condition changes. The time reversal technique has shown to be an effective method to inspect specimens without baseline signals [86,117,121]. It discerns damages by comparing the reconstructed signal to the original signal. The conventional way to evaluate the difference is by building a DI. Instead, the 1DCNN method allows feeding differential signals as input, which removes the need of building a specialized DI according to the testing configuration and specimen properties.

5. Conclusion

In this paper NUT technology for damage characterization is reviewed and is broken down into direct problem and inverse problem. The major conclusions of this review paper can be summarized as follows:

Table 4
Pros and cons of main ML algorithms for different damage characterization tasks.

Characterization tasks	ML algorithms	Pros	Cons	Ref
Damage detection	SVM	• Effective on small dataset • Effective in high dimensional spaces • Computation efficient	• Require expert knowledge to build effective handcrafted features • Sensitive to noise	[27,155]
	ANN	• Capable of finding nonlinear features • Works well on any number of features	• Require expert knowledge to build effective handcrafted features • Computationally expensive than SVM • Needs more training data than SVM	[143,160,161]
	CNN	• Capable of finding complex nonlinear features • Does not require handcrafted features • Robust to noise	• Black boxes, less interpretable • Computationally expensive than ANN • Needs more training data than ANN	[30,171,172]
Damage localization	ANN	• Only needs simple feature extraction process	• Can only predict rough region of damages on specimen	[39,144,163]
	CNN	• Can provide more accurate results than ANN	• Needs more data for training than ANN and Bayesian approach	[31,177]
	Bayesian	• Provide accurate coordinates of damage • Only small scale data for training	• Require solid expert knowledge on NUT,ML, and optimization	[28,190,199]
Damage quantification	ANN/CNN	• Capable of finding nonlinear regression	• Difficult to obtain enough training data	[17,26]

1. The research on direct problems aims to build a physical mechanism of wave-damage interaction considering the material nonlinearity and contact nonlinearity. Two representative schemes of the nonlinear wave-damage interaction model, namely wave-crack in metal and wave-delamination in composites were demonstrated. The material nonlinearity and contact nonlinearity can introduce nonlinear phenomena including higher harmonic generation, sub-harmonic generation, wave modulation, scattering, and mode conversion.
2. The inverse problem of NUT for damage characterization was conducted by performing NUT testing for data acquisition, signal pre-processing for feature extraction, and parameter analysis for damage characterization. NUT techniques include HH, sub-harmonic generation, NWMS, NRUS, and wave mixing were reviewed and the application of NUT techniques for damage characterization was summarized.
3. The state-of-the-art parameter analysis method including DI construction and ML methods for damage characterization was reviewed. In real industrial applications, the mapping between nonlinear features and damage conditions is complicated. In addition, the noises from instruments, measurement, and environment can further complicate the sensory signals and deteriorate the nonlinear features induced by damage. These factors may cause DI-based parameter analysis methods ineffective.
4. ML-enriched parameter analysis methods for damage characterization, including detection, localization, and quantification were systematically reviewed. Compared with CNN, SVM shows relatively good performances for damage detection when the available data for training is small (e.g. 150 samples). ANN has demonstrated good overall performance on all types of damage characterization tasks. However, it requires reasonable handcrafted features varied according to different application scenarios. With more data for training (e.g. 500 samples), CNN can provide a better prediction than ANN in detecting and localizing damage. However, CNN suffers the difficulty in interpreting results for industrial applications. Based on solid statistical analysis, Bayesian inference is capable to reduce uncertainties from measurement and time-varying conditions and shows great potential in providing accurate damage coordinates.
5. Finally, the trends of NUT from the view of data augmentation methods, complex damage characterization applications, and baseline-free methods were discussed.

CRediT authorship contribution statement

Hongguang Yun: Conceptualization, Methodology, Investigation, Resources, Writing – original draft, Visualization. **Rakiba Rayhana:** Investigation, Writing – review & editing. **Shashank Pant:** Conceptualization, Writing – review & editing. **Marc Genest:** Writing – review & editing, Funding acquisition. **Zheng Liu:** Conceptualization, Writing – review & editing, Supervision.

Declaration of competing interest

The authors declare that they have no known competing financial interests or personal relationships that could have appeared to influence the work reported in this paper.

References

[1] C.K. Liew, M. Veidt, N. Rajic, K. Tsoi, D. Rowlands, H. Morton, Inspections of helicopter composite airframe structures using conventional and emerging nondestructive testing methods, J. Test. Eval. 39 (6) (2011) 1011–1022.
[2] G. Dobmann, L. Debarberis, J.-F. Coste, Aging material evaluation and studies by non-destructive techniques (AMES-NDT)—a European network project, Nucl. Eng. Des. 206 (2–3) (2001) 363–374.
[3] W. Wang, A two-stage prognosis model in condition based maintenance, European J. Oper. Res. 182 (3) (2007) 1177–1187.
[4] K.-Y. Jhang, Nonlinear ultrasonic techniques for nondestructive assessment of micro damage in material: a review, Int. J. Precis. Eng. Manuf. 10 (1) (2009) 123–135.
[5] J. Frouin, S. Sathish, T.E. Matikas, J.K. Na, Ultrasonic linear and nonlinear behavior of fatigued Ti–6Al–4V, J. Mater. Res. 14 (4) (1999) 1295–1298.
[6] V.E. Nazarov, A.M. Sutin, Nonlinear elastic constants of solids with cracks, J. Acoust. Soc. Am. 102 (6) (1997) 3349–3354.
[7] J.H. Cantrell, Ultrasonic harmonic generation from fatigue-induced dislocation substructures in planar slip metals and assessment of remaining fatigue life, J. Appl. Phys. 106 (9) (2009) 093516.
[8] M. Meo, U. Polimeno, G. Zumpano, Detecting damage in composite material using nonlinear elastic wave spectroscopy methods, Appl. Compos. Mater. 15 (3) (2008) 115–126.
[9] L. Bjørnø, Forty years of nonlinear ultrasound, Ultrasonics 40 (1–8) (2002) 11–17.
[10] C. Bermes, J.-Y. Kim, J. Qu, L.J. Jacobs, Nonlinear Lamb waves for the detection of material nonlinearity, Mech. Syst. Signal Process. 22 (3) (2008) 638–646.
[11] P. Liu, H. Sohn, T. Kundu, Fatigue crack localization using laser nonlinear wave modulation spectroscopy (LNWMS), J. Korean Soc. Nondestruct. Test. 34 (6) (2014) 419–427.
[12] T. Watanabe, H.T.H. Trang, K. Harada, C. Hashimoto, Evaluation of corrosion-induced crack and rebar corrosion by ultrasonic testing, Constr. Build. Mater. 67 (2014) 197–201.
[13] T. Peng, A. Saxena, K. Goebel, Y. Xiang, S. Sankararaman, Y. Liu, A novel Bayesian imaging method for probabilistic delamination detection of composite materials, Smart Mater. Struct. 22 (12) (2013) 125019.

[14] Q. Wang, S. Ma, D. Yue, Identification of damage in composite structures using Gaussian mixture model-processed Lamb waves, Smart Mater. Struct. 27 (4) (2018) 045007.
[15] M. Todd, E. Flynn, P. Wilcox, B. Drinkwater, A. Croxford, S. Kessler, Ultrasonic wave-based defect localization using probabilistic modeling, in: AIP Conference Proceedings, Vol. 1430, American Institute of Physics, 2012, pp. 639–646.
[16] S. Sharma, A. Mukherjee, Ultrasonic guided waves for monitoring corrosion in submerged plates, Struct. Control Health Monit. 22 (1) (2015) 19–35.
[17] H.J. Lim, H. Sohn, Y. Kim, Data-driven fatigue crack quantification and prognosis using nonlinear ultrasonic modulation, Mech. Syst. Signal Process. 109 (2018) 185–195.
[18] C. Ehrlich, J.-Y. Kim, L. Jacobs, J. Qu, J. Wall, Experimental characterization of creep damage in a welded steel pipe section using a nonlinear ultrasonic technique, in: AIP Conference Proceedings, Vol. 1430, American Institute of Physics, 2012, pp. 292–298.
[19] W. Li, Y. Cho, Thermal fatigue damage assessment in an isotropic pipe using nonlinear ultrasonic guided waves, Exp. Mech. 54 (8) (2014) 1309–1318.
[20] F. Zhong, C. Zhang, W. Li, J. Jiao, L. Zhong, Nonlinear ultrasonic characterization of intergranular corrosion damage in super 304h steel tube, Anti-Corros. Methods Mater. (2016).
[21] A.J. Hunter, B.W. Drinkwater, P.D. Wilcox, Autofocusing ultrasonic imagery for non-destructive testing and evaluation of specimens with complicated geometries, Ndt E Int. 43 (2) (2010) 78–85.
[22] H. Chan, B. Masserey, P. Fromme, High frequency guided ultrasonic waves for hidden fatigue crack growth monitoring in multi-layer model aerospace structures, Smart Mater. Struct. 24 (2) (2015) 025037.
[23] P. Zabbal, G. Ribay, J. Jumel, Nonlinear ultrasound for nondestructive evaluation of adhesive joints, in: AIP Conference Proceedings, Vol. 2102, AIP Publishing LLC, 2019, 020030.
[24] Y. Ren, L. Qiu, S. Yuan, F. Fang, Gaussian mixture model–based path-synthesis accumulation imaging of guided wave for damage monitoring of aircraft composite structures under temperature variation, Struct. Health Monit. 18 (1) (2019) 284–302.
[25] J. Yang, J. He, X. Guan, D. Wang, H. Chen, W. Zhang, Y. Liu, A probabilistic crack size quantification method using in-situ Lamb wave test and Bayesian updating, Mech. Syst. Signal Process. 78 (2016) 118–133.
[26] H.J. Lim, H. Sohn, Online fatigue crack prognosis using nonlinear ultrasonic modulation, Struct. Health Monit. 18 (5–6) (2019) 1889–1902.
[27] S. Agarwal, M. Mitra, Lamb wave based automatic damage detection using matching pursuit and machine learning, Smart Mater. Struct. 23 (8) (2014) 085012.
[28] G. Yan, A Bayesian approach for damage localization in plate-like structures using Lamb waves, Smart Mater. Struct. 22 (3) (2013) 035012.
[29] S. Cantero-Chinchilla, J. Chiachío, M. Chiachío, D. Chronopoulos, A. Jones, A robust Bayesian methodology for damage localization in plate-like structures using ultrasonic guided-waves, Mech. Syst. Signal Process. 122 (2019) 192–205.
[30] N. Munir, H.-J. Kim, J. Park, S.-J. Song, S.-S. Kang, Convolutional neural network for ultrasonic weldment flaw classification in noisy conditions, Ultrasonics 94 (2019) 74–81.
[31] L. Xu, S. Yuan, J. Chen, Y. Ren, Guided wave-convolutional neural network based fatigue crack diagnosis of aircraft structures, Sensors 19 (16) (2019) 3567.
[32] D. Broda, W. Staszewski, A. Martowicz, T. Uhl, V. Silberschmidt, Modelling of nonlinear crack–wave interactions for damage detection based on ultrasound—A review, J. Sound Vib. 333 (4) (2014) 1097–1118.
[33] V. Marcantonio, D. Monarca, A. Colantoni, M. Cecchini, Ultrasonic waves for materials evaluation in fatigue, thermal and corrosion damage: A review, Mech. Syst. Signal Process. 120 (2019) 32–42.
[34] K.H. Matlack, J.-Y. Kim, L.J. Jacobs, J. Qu, Review of second harmonic generation measurement techniques for material state determination in metals, J. Nondestruct. Eval. 34 (1) (2015) 273.
[35] R. Guan, Y. Lu, W. Duan, X. Wang, Guided waves for damage identification in pipeline structures: A review, Struct. Control Health Monit. 24 (11) (2017) e2007.
[36] A. Ghavamian, F. Mustapha, B. Baharudin, N. Yidris, Detection, localisation and assessment of defects in pipes using guided wave techniques: a review, Sensors 18 (12) (2018) 4470.
[37] N. Li, J. Sun, J. Jiao, B. Wu, C. He, Quantitative evaluation of micro-cracks using nonlinear ultrasonic modulation method, Ndt E Int. 79 (2016) 63–72.
[38] J. Cheng, J.N. Potter, A.J. Croxford, B.W. Drinkwater, Monitoring fatigue crack growth using nonlinear ultrasonic phased array imaging, Smart Mater. Struct. 26 (5) (2017) 055006.
[39] B. Feng, D.J. Pasadas, A.L. Ribeiro, H.G. Ramos, Locating defects in anisotropic CFRP plates using ToF-based probability matrix and neural networks, IEEE Trans. Instrum. Meas. 68 (5) (2019) 1252–1260.
[40] J. Paixão, S. da Silva, E. Figueiredo, L. Radu, G. Park, Delamination area quantification in composite structures using Gaussian process regression and auto-regressive models, J. Vib. Control (2020) 1077546320966183.
[41] A.S. Birks, R.E. Green, Nondestructive testing handbook 7: ultrasonic testing, in: ASNT Handbook, 1991.
[42] Z. Su, C. Zhou, M. Hong, L. Cheng, Q. Wang, X. Qing, Acousto-ultrasonics-based fatigue damage characterization: Linear versus nonlinear signal features, Mech. Syst. Signal Process. 45 (1) (2014) 225–239.
[43] B. Le Crom, M. Castaings, Shear horizontal guided wave modes to infer the shear stiffness of adhesive bond layers, J. Acoust. Soc. Am. 127 (4) (2010) 2220–2230.
[44] M. Castaings, Sh ultrasonic guided waves for the evaluation of interfacial adhesion, Ultrasonics 54 (7) (2014) 1760–1775.
[45] S. Shan, M. Hasanian, H. Cho, C.J. Lissenden, L. Cheng, New nonlinear ultrasonic method for material characterization: Codirectional shear horizontal guided wave mixing in plate, Ultrasonics 96 (2019) 64–74.
[46] F.C. Campbell, Elements of Metallurgy and Engineering Alloys, ASM International, 2008.
[47] L.D. Landau, E. Lifshits, Theoretical physics, vol. 7, theory of elasticity, in: Science, Moscow, Main Editorial Board for Physical and Mathematical Literature, 1987.
[48] A.E.H. Love, A Treatise on the Mathematical Theory of Elasticity, Cambridge University Press, 2013.
[49] V. Gusev, V. Tournat, B. Castagnède, Nonlinear acoustic phenomena in micro-inhomogenous media, in: Materials and Acoustics Handbook, Wiley Online Library, 2009, pp. 431–471.
[50] K. Worden, Nonlinearity in Structural Dynamics: Detection, Identification and Modelling, CRC Press, 2019.
[51] P. Gudmundson, The dynamic behaviour of slender structures with cross-sectional cracks, J. Mech. Phys. Solids 31 (4) (1983) 329–345.
[52] M.I. Friswell, J.E. Penny, Crack modeling for structural health monitoring, Struct. Health Monit. 1 (2) (2002) 139–148.
[53] A. Rivola, P. White, Bispectral analysis of the bilinear oscillator with application to the detection of fatigue cracks, J. Sound Vib. 216 (5) (1998) 889–910.
[54] E. Douka, L. Hadjileontiadis, Time–frequency analysis of the free vibration response of a beam with a breathing crack, Ndt E Int. 38 (1) (2005) 3–10.
[55] I.Y. Solodov, N. Krohn, G. Busse, CAN: an example of nonclassical acoustic nonlinearity in solids, Ultrasonics 40 (1–8) (2002) 621–625.
[56] T. Chondros, A. Dimarogonas, J. Yao, Longitudinal vibration of a bar with a breathing crack, Eng. Fract. Mech. 61 (5–6) (1998) 503–518.
[57] T. Chondros, A.D. Dimarogonas, J. Yao, Vibration of a beam with a breathing crack, J. Sound Vib. 239 (1) (2001) 57–67.
[58] A. Sutin, V. Nazarov, Nonlinear acoustic methods of crack diagnostics, Radiophys. Quant. Electron. 38 (3–4) (1995) 109–120.
[59] K.L. Johnson, K.L. Johnson, Contact Mechanics, Cambridge University Press, 1987.
[60] J.A. Greenwood, J.P. Williamson, Contact of nominally flat surfaces, Proc. R. Soc. A 295 (1442) (1966) 300–319.
[61] C.-T. Ng, M. Veidt, Scattering of the fundamental anti-symmetric Lamb wave at delaminations in composite laminates, J. Acoust. Soc. Am. 129 (3) (2011) 1288–1296.
[62] S. Pant, J. Laliberte, M. Martinez, B. Rocha, Derivation and experimental validation of Lamb wave equations for an n-layered anisotropic composite laminate, Compos. Struct. 111 (2014) 566–579.
[63] A.-M. Zelenyak, N. Schorer, M.G. Sause, Modeling of ultrasonic wave propagation in composite laminates with realistic discontinuity representation, Ultrasonics 83 (2018) 103–113.
[64] Y. Yang, C.-T. Ng, A. Kotousov, H. Sohn, H.J. Lim, Second harmonic generation at fatigue cracks by low-frequency Lamb waves: Experimental and numerical studies, Mech. Syst. Signal Process. 99 (2018) 760–773.
[65] M.B. Obenchain, C.E. Cesnik, Guided wave interaction with hole damage using the local interaction simulation approach, Smart Mater. Struct. 23 (12) (2014) 125010.
[66] N. Nanda, Wave propagation analysis of laminated composite shell panels using a frequency domain spectral finite element model, Appl. Math. Model. 89 (2021) 1025–1040.
[67] S. He, C.T. Ng, Modelling and analysis of nonlinear guided waves interaction at a breathing crack using time-domain spectral finite element method, Smart Mater. Struct. 26 (8) (2017) 085002.
[68] R.K. Munian, D.R. Mahapatra, S. Gopalakrishnan, Lamb wave interaction with composite delamination, Compos. Struct. 206 (2018) 484–498.
[69] B.I. Murat, P. Khalili, P. Fromme, Scattering of guided waves at delaminations in composite plates, J. Acoust. Soc. Am. 139 (6) (2016) 3044–3052.
[70] R.K. Munian, D.R. Mahapatra, S. Gopalakrishnan, Ultrasonic guided wave scattering due to delamination in curved composite structures, Compos. Struct. 239 (2020) 111987.
[71] C. Ramadas, K. Balasubramaniam, M. Joshi, C. Krishnamurthy, Interaction of the primary anti-symmetric lamb mode (Ao) with symmetric delaminations: numerical and experimental studies, Smart Mater. Struct. 18 (8) (2009) 085011.
[72] C. Ramadas, K. Balasubramaniam, M. Joshi, C. Krishnamurthy, Interaction of guided Lamb waves with an asymmetrically located delamination in a laminated composite plate, Smart Mater. Struct. 19 (6) (2010) 065009.
[73] X. Gros, NDT Data Fusion, Elsevier, 1996.
[74] D.H. Turnbull, B.G. Starkoski, K.A. Harasiewicz, J.L. Semple, L. From, A.K. Gupta, D.N. Sauder, F.S. Foster, A 40–100 MHz B-scan ultrasound backscatter microscope for skin imaging, Ultrasound Med. Biol. 21 (1) (1995) 79–88.

[75] K. Imielińska, M. Castaings, R. Wojtyra, J. Haras, E. Le Clezio, B. Hosten, Air-coupled ultrasonic C-scan technique in impact response testing of carbon fibre and hybrid: glass, carbon and kevlar/epoxy composites, J. Mater Process. Technol. 157 (2004) 513–522.
[76] L.H. Taylor, F.R. Rollins Jr., Ultrasonic study of three-phonon interactions. I. Theory, Phys. Rev. 136 (3A) (1964) A591.
[77] A.J. Croxford, P.D. Wilcox, B.W. Drinkwater, P.B. Nagy, The use of non-collinear mixing for nonlinear ultrasonic detection of plasticity and fatigue, J. Acoust. Soc. Am. 126 (5) (2009) EL117–EL122.
[78] R. Watkins, R. Jha, A modified time reversal method for Lamb wave based diagnostics of composite structures, Mech. Syst. Signal Process. 31 (2012) 345–354.
[79] C.H. Wang, J.T. Rose, F.-K. Chang, Computerized time-reversal method for structural health monitoring, in: Nondestructive Evaluation and Health Monitoring of Aerospace Materials and Composites II, Vol. 5046, International Society for Optics and Photonics, 2003, pp. 48–58.
[80] H.W. Park, H. Sohn, K.H. Law, C.R. Farrar, Time reversal active sensing for health monitoring of a composite plate, J. Sound Vib. 302 (1–2) (2007) 50–66.
[81] H.W. Park, S.B. Kim, H. Sohn, Understanding a time reversal process in Lamb wave propagation, Wave Motion 46 (7) (2009) 451–467.
[82] P. Blanloeuil, L.F. Rose, M. Veidt, C.H. Wang, Time reversal invariance for a nonlinear scatterer exhibiting contact acoustic nonlinearity, J. Sound Vib. 417 (2018) 413–431.
[83] F. Falcetelli, N. Venturini, M.B. Romero, M.J. Martinez, S. Pant, E. Troiani, Broadband signal reconstruction for SHM: An experimental and numerical time reversal methodology, J. Intell. Mater. Syst. Struct. 32 (10) (2021) 1043–1058.
[84] L. Huang, L. Zeng, J. Lin, Z. Luo, An improved time reversal method for diagnostics of composite plates using Lamb waves, Compos. Struct. 190 (2018) 10–19.
[85] Z. Liu, H. Yu, J. Fan, Y. Hu, C. He, B. Wu, Baseline-free delamination inspection in composite plates by synthesizing non-contact air-coupled Lamb wave scan method and virtual time reversal algorithm, Smart Mater. Struct. 24 (4) (2015) 045014.
[86] J. Wang, Y. Shen, An enhanced Lamb wave virtual time reversal technique for damage detection with transducer transfer function compensation, Smart Mater. Struct. 28 (8) (2019) 085017.
[87] H. Sohn, H.W. Park, K.H. Law, C.R. Farrar, Damage detection in composite plates by using an enhanced time reversal method, J. Aerosp. Eng. 20 (3) (2007) 141–151.
[88] R. Gangadharan, C. Murthy, S. Gopalakrishnan, M. Bhat, Time reversal technique for health monitoring of metallic structure using Lamb waves, Ultrasonics 49 (8) (2009) 696–705.
[89] J.K. Agrahari, S. Kapuria, A refined Lamb wave time-reversal method with enhanced sensitivity for damage detection in isotropic plates, J. Intell. Mater. Syst. Struct. 27 (10) (2016) 1283–1305.
[90] S.V. Walker, J.Y. Kim, J. Qu, L.J. Jacobs, Fatigue damage evaluation in A36 steel using nonlinear Rayleigh surface waves, Ndt E Int. 48 (2012) 10–15.
[91] W.J.N.D. Lima, M.F. Hamilton, Finite-amplitude waves in isotropic elastic plates, J. Sound Vib. 265 (4) (2003) 819–839.
[92] C. Bermes, J.Y. Kim, J. Qu, L.J. Jacobs, Nonlinear Lamb waves for the detection of material nonlinearity, Mech. Syst. Signal Process. 22 (3) (2008) 638–646.
[93] K. Yamanaka, T. Mihara, T. Tsuji, Evaluation of closed cracks by model analysis of subharmonic ultrasound, Japan. J. Appl. Phys. 43 (5S) (2004) 3082.
[94] Y. Ohara, S. Yamamoto, T. Mihara, K. Yamanaka, Ultrasonic evaluation of closed cracks using subharmonic phased array, Japan. J. Appl. Phys. 47 (5S) (2008) 3908.
[95] A. Ouchi, A. Sugawara, Y. Ohara, K. Yamanaka, Subharmonic phased array for crack evaluation using surface acoustic wave, Japan. J. Appl. Phys. 54 (7S1) (2015) 07HC05.
[96] Y. Ohara, Y. Shintaku, S. Horinouchi, M. Ikeuchi, K. Yamanaka, Enhancement of selectivity in nonlinear ultrasonic imaging of closed cracks using amplitude difference phased array, Japan. J. Appl. Phys. 51 (7S) (2012) 07GB18.
[97] M. Zhang, L. Xiao, W. Qu, Y. Lu, Damage detection of fatigue cracks under nonlinear boundary condition using subharmonic resonance, Ultrasonics 77 (2017) 152–159.
[98] D. Ginzburg, F. Ciampa, G. Scarselli, M. Meo, SHM of single lap adhesive joints using subharmonic frequencies, Smart Mater. Struct. 26 (10) (2017) 105018.
[99] J. Jiao, H. Lv, C. He, B. Wu, Fatigue crack evaluation using the non-collinear wave mixing technique, Smart Mater. Struct. 26 (6) (2017) 065005.
[100] J. Jiao, J. Sun, N. Li, G. Song, B. Wu, C. He, Micro-crack detection using a collinear wave mixing technique, Ndt E Int. 62 (2014) 122–129.
[101] M. Liu, G. Tang, L.J. Jacobs, J. Qu, Measuring acoustic nonlinearity parameter using collinear wave mixing, J. Appl. Phys. 112 (2) (2012) 024908.
[102] Y. Zhao, Y. Xu, Z. Chen, P. Cao, N. Hu, Detection and characterization of randomly distributed micro-cracks in elastic solids by one-way collinear mixing method, J. Nondestruct. Eval. 37 (3) (2018) 47.
[103] G. Bunget, S. Henley, C. Glass, J. Rogers, M. Webster, K. Farinholt, F. Friedersdorf, M. Pepi, A. Ghoshal, S. Datta, et al., Decomposition method to detect fatigue damage precursors in thin components through nonlinear ultrasonic with collinear mixing contributions, J. Nondestruct. Eval. Diagn. Progn. Eng. Syst. 3 (2) (2020).
[104] J. Jingpin, S. Junjun, L. Guanghai, W. Bin, H. Cunfu, Evaluation of the intergranular corrosion in austenitic stainless steel using collinear wave mixing method, Ndt E Int. 69 (2015) 1–8.
[105] F. Li, Y. Zhao, P. Cao, N. Hu, Mixing of ultrasonic Lamb waves in thin plates with quadratic nonlinearity, Ultrasonics 87 (2018) 33–43.
[106] W. Li, Y. Xu, N. Hu, M. Deng, Impact damage detection in composites using a guided wave mixing technique, Meas. Sci. Technol. 31 (1) (2019) 014001.
[107] A.K. Metya, S. Tarafder, K. Balasubramaniam, Nonlinear Lamb wave mixing for assessing localized deformation during creep, Ndt E Int. 98 (2018) 89–94.
[108] J. Jingpin, M. Xiangji, H. Cunfu, W. Bin, Nonlinear Lamb wave-mixing technique for micro-crack detection in plates, Ndt E Int. 85 (2017) 63–71.
[109] X. Ding, Y. Zhao, M. Deng, G. Shui, N. Hu, One-way Lamb mixing method in thin plates with randomly distributed micro-cracks, Int. J. Mech. Sci. 171 (2020) 105371.
[110] K.-A. Van Den Abeele, J. Carmeliet, J.A. Ten Cate, P.A. Johnson, Nonlinear elastic wave spectroscopy (NEWS) techniques to discern material damage, Part II: Single-mode nonlinear resonance acoustic spectroscopy, J. Res. Nondestruct. Eval. 12 (1) (2000) 31–42.
[111] C. Payan, V. Garnier, J. Moysan, P. Johnson, Applying nonlinear resonant ultrasound spectroscopy to improving thermal damage assessment in concrete, J. Acoust. Soc. Am. 121 (4) (2007) EL125–EL130.
[112] C. Payan, T.J. Ulrich, P.-Y. Le Bas, T. Saleh, M. Guimaraes, Quantitative linear and nonlinear resonance inspection techniques and analysis for material characterization: Application to concrete thermal damage, J. Acoust. Soc. Am. 136 (2) (2014) 537–546.
[113] K.J. Leśnicki, J.-Y. Kim, K.E. Kurtis, L.J. Jacobs, Characterization of ASR damage in concrete using nonlinear impact resonance acoustic spectroscopy technique, Ndt E Int. 44 (8) (2011) 721–727.
[114] K.J. Leśnicki, J.-Y. Kim, K.E. Kurtis, L.J. Jacobs, Assessment of alkali–silica reaction damage through quantification of concrete nonlinearity, Mater. Struct. 46 (3) (2013) 497–509.
[115] K. Van Den Abeele, P. Le Bas, B. Van Damme, T. Katkowski, Quantification of material nonlinearity in relation to microdamage density using nonlinear reverberation spectroscopy: Experimental and theoretical study, J. Acoust. Soc. Am. 126 (3) (2009) 963–972.
[116] S.M. Hogg, B.E. Anderson, P.-Y. Le Bas, M.C. Remillieux, Nonlinear resonant ultrasound spectroscopy of stress corrosion cracking in stainless steel rods, Ndt E Int. 102 (2019) 194–198.
[117] B. Poddar, C.R. Bijudas, M. Mitra, P.M. Mujumdar, Damage detection in a woven-fabric composite laminate using time-reversed Lamb wave, Struct. Health Monit. 11 (5) (2012) 602–612.
[118] R. Lucena, J. Dos Santos, Structural health monitoring using time reversal and cracked rod spectral element, Mech. Syst. Signal Process. 79 (2016) 86–98.
[119] G. Du, Q. Kong, F. Wu, J. Ruan, G. Song, An experimental feasibility study of pipeline corrosion pit detection using a piezoceramic time reversal mirror, Smart Mater. Struct. 25 (3) (2016) 037002.
[120] Y. Xu, M. Luo, Q. Liu, G. Du, G. Song, PZT transducer array enabled pipeline defect locating based on time-reversal method and matching pursuit de-noising, Smart Mater. Struct. 28 (7) (2019) 075019.
[121] J.K. Agrahari, S. Kapuria, Active detection of block mass and notch-type damages in metallic plates using a refined time-reversed Lamb wave technique, Struct. Control Health Monit. 25 (2) (2018) e2064.
[122] F. Semperlotti, K. Wang, E. Smith, Localization of a breathing crack using super-harmonic signals due to system nonlinearity, AIAA J. 47 (9) (2009) 2076–2086.
[123] S.E. Lee, H.J. Lim, S. Jin, H. Sohn, J.-W. Hong, Micro-crack detection with nonlinear wave modulation technique and its application to loaded cracks, Ndt E Int. 107 (2019) 102132.
[124] C. Zhou, M. Hong, Z. Su, Q. Wang, L. Cheng, Evaluation of fatigue cracks using nonlinearities of acousto-ultrasonic waves acquired by an active sensor network, Smart Mater. Struct. 22 (1) (2012) 015018.
[125] H. Lv, J. Jiao, B. Wu, C. He, Evaluation of fatigue crack orientation using non-collinear shear wave mixing method, J. Nondestruct. Eval. 37 (4) (2018) 74.
[126] B. Feng, A.L. Ribeiro, H.G. Ramos, Interaction of Lamb waves with the edges of a delamination in cfrp composites and a reference-free localization method for delamination, Measurement 122 (2018) 424–431.
[127] B. Poddar, A. Kumar, M. Mitra, P. Mujumdar, Time reversibility of a Lamb wave for damage detection in a metallic plate, Smart Mater. Struct. 20 (2) (2011) 025001.
[128] P. Blanloeuil, L. Rose, J. Guinto, M. Veidt, C. Wang, Closed crack imaging using time reversal method based on fundamental and second harmonic scattering, Wave Motion 66 (2016) 156–176.
[129] X. Zhao, R.L. Royer, S.E. Owens, J.L. Rose, Ultrasonic Lamb wave tomography in structural health monitoring, Smart Mater. Struct. 20 (10) (2011) 105002.
[130] A. Rahbari, M. Rébillat, N. Mechbal, S. Canu, Unsupervised damage clustering in complex aeronautical composite structures monitored by Lamb waves: An inductive approach, Eng. Appl. Artif. Intell. 97 (2021) 104099.
[131] S. Dabetwar, S. Ekwaro-Osire, J.a.P. Dias, Damage classification of composites based on analysis of Lamb wave signals using machine learning, ASCE-ASME J. Risk Uncertain. Eng. Syst. B: Mech. Eng. 7 (1) (2021) 011002.

[132] M. Niethammer, L.J. Jacobs, J. Qu, J. Jarzynski, Time-frequency representations of Lamb waves, J. Acoust. Soc. Am. 109 (5) (2001) 1841–1847.

[133] N.E. Huang, Z. Shen, S.R. Long, M.C. Wu, H.H. Shih, Q. Zheng, N.-C. Yen, C.C. Tung, H.H. Liu, The empirical mode decomposition and the Hilbert spectrum for nonlinear and non-stationary time series analysis, Proc. R. Soc. Lond. Ser. A Math. Phys. Eng. Sci. 454 (1971) (1998) 903–995.

[134] G.K. Sharma, A. Kumar, T. Jayakumar, B. Purnachandra Rao, N. Mariyappa, Ensemble empirical mode decomposition based methodology for ultrasonic testing of coarse grain austenitic stainless steels, Ultrasonics 57 (2015) 167–178.

[135] S.R. Ara, S.K. Bashar, F. Alam, M.K. Hasan, EMD-DWT based transform domain feature reduction approach for quantitative multi-class classification of breast lesions, Ultrasonics 80 (2017) 22–33.

[136] S.G. Mallat, Z. Zhang, Matching pursuits with time-frequency dictionaries, IEEE Trans. Signal Process. 41 (12) (1993) 3397–3415.

[137] C.-b. Xu, Z.-b. Yang, X.-f. Chen, S.-h. Tian, Y. Xie, A guided wave dispersion compensation method based on compressed sensing, Mech. Syst. Signal Process. 103 (2018) 89–104.

[138] F. Boßmann, G. Plonka, T. Peter, O. Nemitz, T. Schmitte, Sparse deconvolution methods for ultrasonic NDT, J. Nondestruct. Eval. 31 (3) (2012) 225–244.

[139] M. Eybpoosh, M. Berges, H.Y. Noh, An energy-based sparse representation of ultrasonic guided-waves for online damage detection of pipelines under varying environmental and operational conditions, Mech. Syst. Signal Process. 82 (2017) 260–278.

[140] H. Gao, Y. Shi, J.L. Rose, Guided wave tomography on an aircraft wing with leave in place sensors, in: AIP Conference Proceedings, Vol. 760, American Institute of Physics, 2005, pp. 1788–1794.

[141] V. Memmolo, N. Pasquino, F. Ricci, Experimental characterization of a damage detection and localization system for composite structures, Measurement 129 (2018) 381–388.

[142] S. Torkamani, S. Roy, M.E. Barkey, E. Sazonov, S. Burkett, S. Kotru, A novel damage index for damage identification using guided waves with application in laminated composites, Smart Mater. Struct. 23 (9) (2014) 095015.

[143] Z. Dworakowski, K. Dragan, T. Stepinski, Artificial neural network ensembles for fatigue damage detection in aircraft, J. Intell. Mater. Syst. Struct. 28 (7) (2017) 851–861.

[144] C. Sbarufatti, G. Manson, K. Worden, A numerically-enhanced machine learning approach to damage diagnosis using a Lamb wave sensing network, J. Sound Vib. 333 (19) (2014) 4499–4525.

[145] X.P. Qing, S. Beard, S.B. Shen, S. Banerjee, I. Bradley, M.M. Salama, F.-K. Chang, Development of a real-time active pipeline integrity detection system, Smart Mater. Struct. 18 (11) (2009) 115010.

[146] S.B. Kotsiantis, I.D. Zaharakis, P.E. Pintelas, Machine learning: a review of classification and combining techniques, Artif. Intell. Rev. 26 (3) (2006) 159–190.

[147] R. Chellappa, C.L. Wilson, S. Sirohey, Human and machine recognition of faces: A survey, Proc. IEEE 83 (5) (1995) 705–741.

[148] D.A. Forsyth, J. Ponce, Computer Vision: A Modern Approach, Prentice Hall Professional Technical Reference, 2002.

[149] C.M. Bishop, Pattern Recognition and Machine Learning, springer, 2006.

[150] K. Virupakshappa, E. Oruklu, Ultrasonic flaw detection using hidden Markov model with wavelet features, in: 2016 IEEE International Ultrasonics Symposium, IUS, IEEE, 2016, pp. 1–4.

[151] Y. Liu, Y.F. Zheng, One-against-all multi-class SVM classification using reliability measures, in: Proceedings. 2005 IEEE International Joint Conference on Neural Networks, 2005, Vol. 2, IEEE, 2005, pp. 849–854.

[152] G. Madzarov, D. Gjorgjevikj, I. Chorbev, A multi-class SVM classifier utilizing binary decision tree, Informatica 33 (2) (2009).

[153] S. Das, A. Chattopadhyay, A.N. Srivastava, Classifying induced damage in composite plates using one-class support vector machines, AIAA J. 48 (4) (2010) 705–718.

[154] F. Sun, N. Wang, J. He, X. Guan, J. Yang, Lamb wave damage quantification using GA-based LS-SVM, Materials 10 (6) (2017) 648.

[155] Z. Zhang, H. Pan, X. Wang, Z. Lin, Machine learning-enriched Lamb wave approaches for automated damage detection, Sensors 20 (6) (2020) 1790.

[156] Y. Lei, B. Yang, X. Jiang, F. Jia, N. Li, A.K. Nandi, Applications of machine learning to machine fault diagnosis: A review and roadmap, Mech. Syst. Signal Process. 138 (2020) 106587.

[157] D.E. Rumelhart, G.E. Hinton, R.J. Williams, Learning representations by back-propagating errors, Nature 323 (6088) (1986) 533–536.

[158] S. Legendre, D. Massicotte, J. Goyette, T.K. Bose, Neural classification of Lamb wave ultrasonic weld testing signals using wavelet coefficients, IEEE Trans. Instrum. Meas. 50 (3) (2001) 672–678.

[159] G. Simone, F.C. Morabito, R. Polikar, P. Ramuhalli, L. Udpa, S. Udpa, Feature extraction techniques for ultrasonic signal classification, Int. J. Appl. Electromagn. Mech. 15 (1–4) (2002) 291–294.

[160] Z. Su, L. Ye, Lamb wave-based quantitative identification of delamination in CF/EP composite structures using artificial neural algorithm, Compos. Struct. 66 (1–4) (2004) 627–637.

[161] Y. Lu, L. Ye, Z. Su, L. Zhou, L. Cheng, Artificial neural network (ANN)-based crack identification in aluminum plates with Lamb wave signals, J. Intell. Mater. Syst. Struct. 20 (1) (2009) 39–49.

[162] P. Nazarko, L. Ziemianski, Damage detection in aluminum and composite elements using neural networks for Lamb waves signal processing, Eng. Fail. Anal. 69 (2016) 97–107.

[163] A. De Fenza, A. Sorrentino, P. Vitiello, Application of artificial neural networks and probability ellipse methods for damage detection using Lamb waves, Compos. Struct. 133 (2015) 390–403.

[164] G. Hinton, L. Deng, D. Yu, G.E. Dahl, A.-r. Mohamed, N. Jaitly, A. Senior, V. Vanhoucke, P. Nguyen, T.N. Sainath, et al., Deep neural networks for acoustic modeling in speech recognition: The shared views of four research groups, IEEE Signal Process. Mag. 29 (6) (2012) 82–97.

[165] Y. LeCun, L. Bottou, Y. Bengio, P. Haffner, Gradient-based learning applied to document recognition, Proc. IEEE 86 (11) (1998) 2278–2324.

[166] T. Wang, D.J. Wu, A. Coates, A.Y. Ng, End-to-end text recognition with convolutional neural networks, in: Proceedings of the 21st International Conference on Pattern Recognition, ICPR2012, IEEE, 2012, pp. 3304–3308.

[167] K. He, X. Zhang, S. Ren, J. Sun, Deep residual learning for image recognition, in: Proceedings of the IEEE Conference on Computer Vision and Pattern Recognition, 2016, pp. 770–778.

[168] A. Khan, A. Sohail, U. Zahoora, A.S. Qureshi, A survey of the recent architectures of deep convolutional neural networks, Artif. Intell. Rev. 53 (8) (2020) 5455–5516.

[169] A. Krizhevsky, I. Sutskever, G.E. Hinton, Imagenet classification with deep convolutional neural networks, Adv. Neural Inf. Process. Syst. 25 (2012) 1097–1105.

[170] M.D. Zeiler, R. Fergus, Visualizing and understanding convolutional networks, in: European Conference on Computer Vision, Springer, 2014, pp. 818–833.

[171] M. Meng, Y.J. Chua, E. Wouterson, C.P.K. Ong, Ultrasonic signal classification and imaging system for composite materials via deep convolutional neural networks, Neurocomputing 257 (2017) 128–135.

[172] J. Melville, K.S. Alguri, C. Deemer, J.B. Harley, Structural damage detection using deep learning of ultrasonic guided waves, in: AIP Conference Proceedings, Vol. 1949, AIP Publishing LLC, 2018, 230004.

[173] H. Liu, Y. Zhang, Deep learning based crack damage detection technique for thin plate structures using guided Lamb wave signals, Smart Mater. Struct. 29 (1) (2019) 015032.

[174] C. Su, M. Jiang, S. Lv, S. Lu, L. Zhang, F. Zhang, Q. Sui, Improved damage localization and quantification of CFRP using Lamb waves and convolution neural network, IEEE Sens. J. 19 (14) (2019) 5784–5791.

[175] V. Suresh, P. Janik, J. Rezmer, Z. Leonowicz, Forecasting solar PV output using convolutional neural networks with a sliding window algorithm, Energies 13 (3) (2020) 723.

[176] A. Rai, M. Mitra, Lamb wave based damage detection in metallic plates using multi-headed 1-dimensional convolutional neural network, Smart Mater. Struct. 30 (3) (2021) 035010.

[177] S. Zhang, C.M. Li, W. Ye, Damage localization in plate-like structures using time-varying feature and one-dimensional convolutional neural network, Mech. Syst. Signal Process. 147 (2021) 107107.

[178] T. Ince, S. Kiranyaz, L. Eren, M. Askar, M. Gabbouj, Real-time motor fault detection by 1-D convolutional neural networks, IEEE Trans. Ind. Electron. 63 (11) (2016) 7067–7075.

[179] S. Wold, K. Esbensen, P. Geladi, Principal component analysis, Chemometr. Intell. Lab. Syst. 2 (1–3) (1987) 37–52.

[180] L. Bai, A. Velichko, B.W. Drinkwater, Characterization of defects using ultrasonic arrays: a dynamic classifier approach, IEEE Trans. Ultrason. Ferroelectr. Freq. Control 62 (12) (2015) 2146–2160.

[181] C. Miao, Y. Wang, Y. Zhang, J. Qu, M.J. Zuo, X. Wang, A SVM classifier combined with PCA for ultrasonic crack size classification, in: 2008 Canadian Conference on Electrical and Computer Engineering, IEEE, 2008, pp. 001627–001630.

[182] L. Qiu, S. Yuan, Q. Bao, H. Mei, Y. Ren, Crack propagation monitoring in a full-scale aircraft fatigue test based on guided wave-Gaussian mixture model, Smart Mater. Struct. 25 (5) (2016) 055048.

[183] L. Qiu, F. Fang, S. Yuan, Improved density peak clustering-based adaptive Gaussian mixture model for damage monitoring in aircraft structures under time-varying conditions, Mech. Syst. Signal Process. 126 (2019) 281–304.

[184] S. Lloyd, Least squares quantization in PCM, IEEE Trans. Inform. Theory 28 (2) (1982) 129–137.

[185] A. Singh, A. Yadav, A. Rana, K-means with three different distance metrics, Int. J. Comput. Appl. 67 (10) (2013).

[186] A.E. Bouzenad, M. El Mountassir, S. Yaacoubi, F. Dahmene, M. Koabaz, L. Buchheit, W. Ke, et al., A semi-supervised based k-means algorithm for optimal guided waves structural health monitoring: A case study, Inventions 4 (1) (2019) 17.

[187] C. Andrieu, N. De Freitas, A. Doucet, M.I. Jordan, An introduction to MCMC for machine learning, Mach. Learn. 50 (1) (2003) 5–43.

[188] X. Zhao, H. Gao, G. Zhang, B. Ayhan, F. Yan, C. Kwan, J.L. Rose, Active health monitoring of an aircraft wing with embedded piezoelectric sensor/actuator network: I. Defect detection, localization and growth monitoring, Smart Mater. Struct. 16 (4) (2007) 1208.

[189] C.-T. Ng, BayesIan model updating approach for experimental identification of damage in beams using guided waves, Struct. Health Monit. 13 (4) (2014) 359–373.
[190] C. Fendzi, N. Mechbal, M. Rebillat, M. Guskov, G. Coffignal, A general Bayesian framework for ellipse-based and hyperbola-based damage localization in anisotropic composite plates, J. Intell. Mater. Syst. Struct. 27 (3) (2016) 350–374.
[191] S. He, C.-T. Ng, A probabilistic approach for quantitative identification of multiple delaminations in laminated composite beams using guided waves, Eng. Struct. 127 (2016) 602–614.
[192] S. He, C.-T. Ng, Guided wave-based identification of multiple cracks in beams using a Bayesian approach, Mech. Syst. Signal Process. 84 (2017) 324–345.
[193] H. Reed, C.A. Leckey, A. Dick, G. Harvey, J. Dobson, A model based bayesian solution for characterization of complex damage scenarios in aerospace composite structures, Ultrasonics 82 (2018) 272–288.
[194] H. Huo, J. He, X. Guan, A Bayesian fusion method for composite damage identification using Lamb wave, Struct. Health Monit. (2020) 1475921720945000.
[195] D. Wang, J. He, X. Guan, J. Yang, W. Zhang, A model assessment method for predicting structural fatigue life using Lamb waves, Ultrasonics 84 (2018) 319–328.
[196] B. Wu, Y. Huang, X. Chen, S. Krishnaswamy, H. Li, Guided-wave signal processing by the sparse Bayesian learning approach employing Gabor pulse model, Struct. Health Monit. 16 (3) (2017) 347–362.
[197] C. Xu, Z. Yang, B. Qiao, X. Chen, Traveling distance estimation for dispersive Lamb waves through sparse Bayesian learning strategy, Smart Mater. Struct. 28 (8) (2019) 085008.
[198] C. Xu, Z. Yang, B. Qiao, X. Chen, A parameter estimation based sparse representation approach for mode separation and dispersion compensation of Lamb waves in isotropic plate, Smart Mater. Struct. 29 (3) (2020) 035020.
[199] M. Zhao, W. Zhou, Y. Huang, H. Li, Sparse Bayesian learning approach for propagation distance recognition and damage localization in plate-like structures using guided waves, Struct. Health Monit. 20 (1) (2021) 3–24.
[200] G. Tripathi, H. Anowarul, K. Agarwal, D.K. Prasad, Classification of micro-damage in piezoelectric ceramics using machine learning of ultrasound signals, Sensors 19 (19) (2019) 4216.
[201] S. Guan, X. Wang, L. Hua, L. Li, Quantitative ultrasonic testing for near-surface defects of large ring forgings using feature extraction and GA-SVM, Appl. Acoust. 173 (2021) 107714.
[202] K. Weiss, T.M. Khoshgoftaar, D. Wang, A survey of transfer learning, J. Big Data 3 (1) (2016) 1–40.